Title
Role of Adult Stem Cells in Tissue Remodeling and Diseases

Author
Tang, Zhenyu

Publication Date
2012

Peer reviewed|Thesis/dissertation

Role of Adult Stem Cells in Tissue Remodeling and Diseases

by

Zhenyu Tang

A dissertation submitted in partial satisfaction of the

requirements for the degree of

Joint Doctor of Philosophy
with University of California, San Francisco

in

Bioengineering

in the

Graduate Division

of the

University of California, Berkeley

Committee in Charge:

Professor Song Li, Chair
Professor William L. Young
Professor Lin He
Professor Xiaohua Gong

Fall, 2012

Role of Adult Stem Cells in
Tissue Remodeling and Diseases

by

Zhenyu Tang

Abstract

Role of Adult Stem Cells in Tissue Remodeling and Diseases

by

Zhenyu Tang

Joint Doctor of Philosophy

with University of California, San Francisco

in Bioengineering

University of California, Berkeley

Professor Song Li, Chair

Tissue specific adult stem cells can be isolated from various tissues and show great capacity of self-renewal and multipotency, thus making it a valuable cell source for regenerative medicine. However, despite its function in homeostasis and tissue repair, it is not clear whether normal adult stem cells could be involved in diseases, like cancer stem cells. Therefore, we investigated this issue in the cardiovascular system, wound healing model and knee joint system. Cardiovascular disease is the number one killer worldwide, which is responsible for approximately 40% of annual deaths in United States. Although various vascular stem cells and progenitor cells were isolated from blood vessel wall, it is not clear whether and how these stem cells contribute to diseases. In the general wound healing, although bone marrow cells and hematopoietic stem cells were identified as the sources of myofibroblasts, which are generally believed to be the culprit of scar tissue formation, it is not clear whether local tissue specific stem cells could be another source of myofibroblasts. In knee joint, osteoarthritis represents structural breakdown of the synovial joint, affecting 70 million people in the United States. However previous identified synovial stem cells are only characterized by non-specific surface markers and their response to biomaterials are not well understood. Therefore, in this dissertation work, we will address these fundamental issues to elucidate the role of adult stem cells in tissue remodeling and diseases.

It is generally accepted that the de-differentiation of smooth muscle cells (SMCs) from contractile to proliferative or synthetic phenotype plays an important role during vascular remodeling and diseases. In the first 3 chapters,

we provide evidence that challenges this dogma. We identify a new type of multipotent vascular stem cell (MVSC) in blood vessel wall. MVSCs express markers including Sox17, Sox10 and S100β, are cloneable, have telomerase activity, and can differentiate into neural cells and mesenchymal stem cell (MSC)-like cells that subsequently differentiate into SMCs. On the other hand, we use lineage tracing with smooth muscle myosin heavy chain (SM-MHC) as a marker to show that MVSCs and proliferative or synthetic SMCs do not arise from the de-differentiation of mature SMCs. Upon vascular injuries, MVSCs, instead of SMCs, become proliferative, and MVSCs can differentiate into SMCs and chondrogenic cells, thus contributing to vascular remodeling and neointimal hyperplasia. Moreover, we also isolated MVSCs from neointima and plaque from patients with atherosclerosis. These findings support a new hypothesis that the differentiation of MVSCs rather than the de-differentiation of SMCs contributes to vascular remodeling and diseases. The MVSCs instead of SMCs should be treated as the targets for drug screening and development.

In the second part of the work, we investigated the general wound healing process and remodeling of implanted artificial biomaterials. It is generally accepted that myofibroblasts play a retractile role in wound contraction and are involved in the synthesis of extracellular matrix components to form the scar tissues. We performed detailed characterization and found a novel type of stem cells showing similar feature with MVSCs, which express markers including Sox10, Sox17 and S100β, can spontaneously differentiate into myofibroblasts and eventually SMCs. *In vivo* studies also identified $Sox10^+$ cells at early stage of wound healing, remodeling of vascular grafts and implanted biomaterials. This work identified a new precursor of myofibroblasts and provided new tools for further research.

In the last part, we identified and characterized a new type of stem cells from the synovial membrane of knee joint, named neural crest cell-like synovial stem cells (NCCL-SSCs). NCCL-SSCs showed the characteristics of neural crest stem cells: they expressed markers such as Sox10, Sox17 and S100β, were clonable, and could differentiate into neural lineages as well as mesenchymal lineages. However, lineage tracing with Wnt-1 as marker showed that NCCL-SSCs were not derived from neural crest. When treated with transforming growth factor β1 (TGF-β1), NCCL-SSCs differentiated into MSCs, lost the expression of Sox17, and lost the differentiation potential into neural lineages, but retained the potential of differentiating into mesenchymal lineages. To determine the responses of NCCL-SSCs to microfibrous scaffolds for tissue engineering, electrospun composite scaffolds with various porosities were fabricated by co-electrospinning of structural and sacrificial microfibers. Interestingly, microfibrous scaffolds with higher porosity increased the expression of chondrogenic and osteogenic genes but suppressed smooth

muscle and adipogenic genes. These results suggest that NCCL-SSCs have tremendous potential for tissue engineering and their differentiation can be controlled by both soluble chemical factors and the biophysical factors such as the porosity of the scaffold.

In summary, this dissertation work identified new tissue specific adult stem cells and performed detailed characterization. This work demonstrated the role of adult stem cells in vascular diseases and scar formation for the first time, indicating that many diseases might be stem cell diseases like cancer. Stem cells instead of somatic cells might be the target for the design of novel therapeutic strategy. Furthermore, we also provide new insight into the response of stem cells on physical properties of biomaterials, thus providing guidance for the design of suitable scaffolds for tissue engineering. We hope this dissertation work could promote the research in investigating the function of stem cells in not only regenerative medicine, but also diseases, thus contributing to our healthcare system.

Acknowledgements

My official studies in Berkeley will be over after this dissertation work, but my intimacy with all the friends here just starts. In retrospect, I feel like the four year's life here is like a beautiful dream, although I am desperate to graduate to start my own career just like seven years ago when I finished my studies in college. The difference is that I do believe I am ready now to fight for my ultimate goal because of the knowledge, the glories, and more importantly, the confidence I was endowed in Berkeley. I would like to take this opportunity to thank all my friends because I would not be where I am without the help of them.

First I would like to thank professor Song Li for being such a great mentor. I won't be in such a fantastic graduate school without the help from him. I used to have trouble in my study because of the language and culture barriers. But his patience and help made me a good researcher, a confident person and an ambitious leader. I am very glad that his help and guidance will still be with me in my future career. I would also like to thank my three other committee members, Dr. William Young, Dr. Lin He and Dr. Xiaohua Gong, for their excellent assistance in my research.

Besides my mentors, I really appreciate the help, laughter and a lot of fun from the Li lab members such as Aijun Wang, Benjamin Lee, Dong Wang, Zhiqiang Yan, Jian Yu and Zoey Huang. A special thanks to the Li lab manager, Julia Chu for here excellent technical assistance and kind help. I would also like to thank Mary West in QB3/CIRM shared facility for her patience and guidance on so many experiments. I cannot finish my dissertation work so fast without the help from them.

Most importantly, I would like to thank my family for their support and love for so many years. Daddy, thank you for your guidance, company and love since I was a child and congratulations on your new movie!!! I'm looking forward to seeing it with everyone. Mom, thanks for your love and support during my 23 years' life in school. I will take the responsibility of taking care of our family from now on. Yanli, I have been the luckiest man in the world because of you. Thanks for accompanying me and waiting for me during my endless lab work in Berkeley. I really appreciate your tolerance, patience and understanding. I love you. I love all of you.

Table of contents

Chapter 1. Introduction

1.1 Cardiovascular disease

Cardiovascular disease (CVD) is the number one killer worldwide, which is responsible for approximately 40% of annual deaths in United States. Furthermore, CVD can also cause significant long-term disability from the complications[1]. The estimated cost due to CVD-related disorders amounts to $330 billion and the American Heart Association spent $380 million annually on CVD research[2]. Currently, the causes of CVD are diverse but atherosclerosis represents the most common ones.

Atherosclerosis gives rise to cerebrovascular disease and CAD through a slowly progressing lesion formation and luminal narrowing of arteries. The endothelial dysfunction and structural alterations, including the absence of a confluent elastin layer and exposure of proteoglycans, which permit sub-endothelial accumulation of low-density lipoprotein (LDL), are believed to be the initial events[3]. The expression of adhesion molecules and the secretion of chemokines by endothelial cells triggered by oxidized lipids and LDL, together with the deposition of platelet-derived chemokines, drive intimal immune cell infiltration. Then a necrotic core is formed by successive accumulation of apoptotic cells, debris and cholesterol crystals, followed by the formation of a fibrous cap composed of collagen and smooth muscle cells (SMCs) to cover the fibroatheromatous plaques[4].

Angioplasty is a common procedure which allows the endovascular treatment of occlusive coronary artery disease without the need of bypass surgery. Briefly, this procedure is executed by attaching a small balloon to a catheter, which dilates the artery and improves blood flow once inflated on the stenosis. In addition, to prevent acute occlusion, vascular recoil and eventually restenosis due to uncontrollable plaque disruption by angioplasty, stents that are metal mesh tubes placed during percutaneous intervention inside the artery to keep arteries open were developed between 1980s and 1990s. However, late in-stent restenosis is still one of the major drawbacks after successful revascularization[5]. The neointimal hyperplasia is the major pathogenic event of in-stent restenosis[6]. It is generally believed that the intimal hyperplasia takes place in concert with the migration of vascular SMCs from tunica media of blood vessel wall after disruption of endothelial barrier following the mechanical stretch. The proliferation of SMCs actively gives rise to neointima and obstructs the vessel. At a later stage, extra-cellular matrix components including proteoglycans and collagen become the predominant constituents of restenotic lesions.

1.2 Phenotypic modulation of SMCs

In native blood vessel wall, the highly specialized contractile SMCs are thought to be the only cell type in tunica media, which are characterized by the

cytoplasm largely filled with thick and thin myofilaments. The principle function of SMCs is contraction and regulation of blood vessel tone-diameter, blood pressure and blood flow distribution[7]. Mature SMCs proliferate at an extremely low rate, exhibit very low synthetic activity and express unique contractile proteins including smooth muscle myosin heavy chain (SM-MHC) and calponin-1 (CNN1) required for the cell's contractile function[8]. However, after cell isolation, the cells barely grew in the first week of the primary culture followed by a sudden cell expansion afterwards. Numerous studies showed that the expandable cell population expresses the markers of immature SMC such as smooth muscle α–actin (SMA), CNN1 and SM-22α, which appears to suggest that these cells are derived from mature SMCs. Therefore, a correlative hypothesis suggests that SMCs can modulate their phenotype and become proliferative[9]. Similarly, the conclusion on the phenotypic modulation of SMCs *in vivo* was also mostly based on the assumption that the cells in injured arteries are mostly derived from SMCs. For examples, one of the classical studies showed that, following artery ligation, the cells in the neointima have synthetic phenotype and differed from SMCs in ultrastructure, which were assumed to be de-differentiated SMCs[10]. However, so far there is no direct evidence to prove this hypothesis. Rigorous lineage tracing experiments are required to directly trace the fate of SMCs.

1.3 Cell marking by genetic recombination

Genetic recombination was first used for lineage tracing since the early 1990s and is now the preferred approach in many experiments. A recombinase enzyme is expressed in a cell- or tissue-specific manner to activate the expression of a conditional reporter gene, and thus allowing for permanent genetic labeling of all progeny of the marked cells. In mice, the genetic lineage tracing is usually performed by using the Cre-loxP system adapted from bacteriophage P1[11]. Briefly, Cre recombinase is expressed under the control of a tissue- or cell-specific promoter in one mouse line. That line is crossed with a second mouse line in which a reporter is flanked by a loxP-STOP-loxP sequence. In animals expressing both constructs, Cre specifically activates the reporter in cells that express the promoter, by excising the STOP sequence.

By using SM22α Cre dependent lineage tracing, it was reported that SMCs give rise to osteochondrogenic cells within calcified arterial media, as well as atherosclerotic lesions[12]. In addition, Owens *et al.* utilized another novel transgenic mouse harboring a SM-22α-LacZ reporter gene containing a mutated G/C repressor element, which faithfully recapitulates expression of endogenous SM22α gene throughout development and maturation[13]. Regen *et al.* observed $LacZ^{+}$ phenotypically-modulated SMCs in the media and neointima 7 days after the carotid wire injury[14]. Furthermore, Wamhoff *et al.* showed a high frequency of proliferating intimal SMCs within lesions of Western diet ApoE-/- mice using the SM22α G/C repressor lineage tracing mouse model[15]. However, SM-22α is also expressed in many other types of

cells in blood vessels including adventitia myofibroblasts[16] and activated macrophages[17], thus compromising the conclusion on SMC de-differentiation and trans-differentiation.

1.4 Nanofibrous scaffolds for cell transplantation

Native extracellular matrix (ECM) has fibril structure. For example, blood vessel wall is composed of ECM fibrils such as collagen and elastin. To simulate the native ECM micro/nano structure, we have used electrospinning technique to fabricate nanofibrous scaffolds with random or aligned nanofibers (500-800 nm in fiber diameter) by using many types of biopolymers[18,19,20]. Nanofibrous tubular scaffolds were used as either vascular grafts or nerve conduits in our *in vivo* studies. The electrospinning process is realized by applying a high-voltage electric field to drive the jet flow of polymer solution from a needle (spinneret). As the jet stream of polymer solution reaches a grounded target (e.g., rotating mandrel), the jet stream can be collected as an interconnected web of fine sub-micron size fibers. We have established a novel method to fabricate nanofibrous conduits with aligned nanofibers on the luminal surface [21].

We have a well established rat model for vascular graft implantation[20,22]. This model can be used to investigate the role of stem cells in vascular graft remodeling. Recently, we developed a method to seed large number of cells on the outer surface of nanofibrous vascular grafts[23]. Cells were embedded in collagen gel on the outer surface of the graft, and cell contraction compacted the gel tightly to the outer surface. The gel has the advantage of maintaining a stable microenvironment for implanted cells, e.g., keep cell survival and avoid cell detachment and dehydration during implantation process.

We have also established an *in vivo* model to investigate peripheral nerve regeneration[24]. A nanofibrous nerve conduit can be used to bridge the transected rat sciatic nerve with a 1-cm gap. The conduit is sutured to nerve stumps at proximal and distal ends. To determine the effects of stem cells on peripheral nerve regeneration, nerve conduits were filled with matrigel only or with cells/matrigel in the lumen.

1.5 Myofibroblasts and wound Healing

It is well known that inflammatory process begins immediately after injury. Then platelets participating into clot formation release chemotatic factors to attract leukocytes, endothelial cells and fibroblasts. Soon after clot formation, granulation tissue begins to form and myofibroblasts in granulation tissues are characterized by similar ultrastructural and biochemical features of SMCs, including the presence of microfilament bundles and the expression of SMA[25]. It is generally accepted that myofibroblasts play a retractile role in wound contraction and are implicated in the synthesis of ECM components such as tenascin, fibronectin, and collagens I and III to replace damaged

tissues. After the wound healing process, myofibroblasts disappear by apoptosis and the scar tissue becomes less cellular and composed of typical fibroblasts. Drugs targeting myofibroblastic differentiation and granulation tissue formation are generally used to decrease scar formation[26].

Despite the importance of myofibroblasts in wound healing and scar formation, the origins of myofibroblasts are still controversial. Friendenstein and associates provided *in vitro* evidence for a bone marrow origin 3 decades ago[27]. They identified colonies consisting of fibroblasts in bone marrow, which can spontaneously differentiate into myofibroblasts in medium with fetal bovine serum (FBS)[28]. However, the model of epithelial-mesenchymal transition (EMT) based on studies in developmental biology suggests organ epithelium origin of myofibroblasts[29]. Furthermore, by transplanting clones derived from single hematopoietic stem cell (HSCs) expressing transgenic enhanced GFP, Ogawa *et al*. found that fibroblasts/myofibroblasts in many organs and tissues are derived from HSCs[30]. To date, it is not clear whether there are other origins of myofibroblasts in wound healing and tissue regeneration.

1.6 Osteoarthritis and stem Cells

Osteoarthritis represents structural breakdown of the synovial joint, affecting 70 million people in the United States[31]. Therefore, efficient therapeutic methodology for tissue regeneration, including cartilage, bone, adipose tissue and tendon has become an urgent need in clinical application. Mesenchymal stem cells (MSCs) have been isolated from synovial membrane and show potential for bone, tendon and cartilage tissue engineering[32]. In addition, bioactive scaffolds were used for efficient *in situ* cartilage regeneration by chemotactic homing of synovial stem cells by delivery of transforming growth factor β-3 (TGF-β3) and stromal cell derived factor-1 (SDF-1) [33,34], thus making local stem cells a great cell source for knee joint repair. However, the characterization of synovial MSCs is limited to non-specific surface markers including CD29 and CD44. In addition, the culture condition relies on high concentrations of serum, which might not be perfect to maintain self-renewal and multipotency of stem cells.

1.7 Porosity of scaffold and response of stem cells

There exist numerous scaffold fabrication techniques aimed to produce artificial environment necessary for tissue engineering. Electrospinning is a highly versatile method that allows the fabrication of biomimetic porous, nonwoven and three-dimensional (3D) fiber structures with controllable fiber diameter ranging from nano- to micro-scale [35,36], and thus has been used extensively in bone, cartilage, tendon, adipose tissue and muscle tissue engineering [37,38]. However, one main problem of electrospun scaffolds that has yet to be solved is their porosity. Moreover, the effects of the pore size of scaffolds on stem cell behaviors are not well understood. We co-electrospun

two synthetic biodegradable polyesters with different degradation rates, poly(L-lactide) (PLLA) and polyglycolic acid (PGA), to fabricate composite scaffolds containing various numbers of PGA fibers; these sacrificial PGA fibers were subsequently removed by short-term degradation of 2 weeks and 4 weeks *in vitro*, demonstrating that such controlled degradation and the selective time-dependent removal of these sacrificial fibers effectively improved the porosity of our composite scaffolds. The responses of tissue specific stem cells to the porosity of scaffolds were investigated in this dissertation work.

Chapter 2. Identification of multipotent vascular stem cells

2.1 Motivation

Since there is no direct evidence to show that the fast growing cells in culture or in neointima after vascular injury are derived from de-differentiation of contractile SMCs, it is reasonable to raise the question: Is it possible that the fast growing cells are derived from a minority population of stem cells in blood vessel wall? In addition, previous studies showed that cultured SMCs can be induced to undergo an osteochondrogenic phenotype characterized by the loss of SMC markers and gain of osteochondrogenic markers (Runx1/Cbfa1, osteopontin and osteocalcin)[39]. Furthermore, it was reported that SMCs give rise to osteochondrogenic cells within calcified arterial media, as well as atherosclerotic lesions by using SM22α Cre dependent lineage tracing[12]. Overall, we hypothesized that there may exist a stem cell population in the blood vessel wall. After cell isolation, these stem cells proliferate rapidly to dominate the culture and give rise to previously reported proliferative or synthetic SMCs. To test this hypothesis, we performed cell isolation from tunica media of rat blood vessel tissues and identified multipotent vascular stem cells (MVSCs).

2.2 Methods and materials

Cell Isolation

Cells were isolated from the blood vessels of Sprague Dawley (SD) rat. The cell isolation methods were described previously[40]. Briefly, the tissue segments were washed three times with PBS supplemented with 1% penicillin/streptomycin (P/S). The surrounding connective tissues and adventitia were dissected away under a dissecting microscope. Endothelium was removed by scraping off the cell layer on the luminal surface with sterile scalpel blades. For tissue explant culture method, the tunica media was cut into mm size and placed onto the surface coated with 1% CellStart (Invitrogen) in 6-well plates. The cells were cultured in DMEM with 10% FBS (Thermo Fisher Scientific), or in DMEM with 2% chick embryo extract (CEE) (MP Biomedical), 1% FBS, 1% N2 (Invitrogen), 2% B27 (Invitrogen), 100 nM retinoic acid (Sigma-Aldrich), 50 nM 2-mercaptoethanol (2ME) (Sigma-Aldrich), 1% P/S and 20 ng/ml basic fibroblast growth factor (bFGF) (Peprotech) (maintenance medium). For enzymatic digestion method, tissues were incubated with 3 mg/ml type II collagenase (Sigma-Aldrich) in DMEM with a 1/5 (w/v) ratio of tissue (g) to enzyme solution (ml). After incubation at 37 °C for 30 min, the same volume of 1 mg/ml elastase (Sigma-Aldrich) solution was added to the solution containing the tissue and collagenase. The tissues were incubated for another 1–2 hours until all the tissues were digested. Cells were then seeded onto CellStart coated dishes and maintained at 37 °C in an

incubator with 5% CO_2.

Cell cloning assays

For the clonal assays, MVSCs were detached, and the cells were resuspended with maintenance medium and filtered through membranes with 40-μm pore size to obtain single cells. Filtered cells were seeded onto CellStart coated 96-well plates at the clonal density (1 cell per well) and cultured for 3 weeks at 37 °C in an incubator with 5% CO_2.

Sphere formation and differentiation assays

For sphere formation assay, cell suspension was plated onto ultralow-attachment 6-well plates (Corning) at the density of 0.5×10^6 cells per well in the presence of maintenance medium for 1 week. The derived neural sphere-like aggregates were collected and embedded into optimal cutting temperature (OCT) compound (Tissue Tek) for cryosectioning and immunostaining. For the directed differentiation of MVSCs into peripheral neurons, Schwann cells, osteoblasts, adipocytes and chondrocytes, the cells were incubated in specific induction media, described previously, for 1–3 weeks[23,24,41].

Telomerase activity assay

Telomerase activities of MVSCs and the tissues from which the cells were isolated were measured using telomeric repeats amplification protocol combined with real-time detection of amplification products, using a Quantitative Telomerase Detection kit (US Biomax), according to the instruction of the manufacturer. Total protein extract (0.5 μg for each sample) was used in each reaction. Real-time PCR analysis was performed using an ABI PRISM 7,000 Sequence Detection System. The amount of molecules was quantified using the standard curve, and normalized with the level of actin in each sample measured by an ELISA kit (Cell Signaling Technology).

Growth factor treatment and cell proliferation assay

Undifferentiated MVSCs and partially differentiated MVSCs (cultured in DMEM with 10% FBS for 3 weeks) were starved in DMEM with 1% FBS for 24 hours followed by the treatment of 10 ng/ml bFGF, 10 ng/ml platelet derived growth factor-B (PDGF-B) (Peprotech) or 10 ng/ml transforming growth factor beta 1 (TGF-β1) (Peprotech) for another 24 hours. The cell proliferation was quantified using Click-iT EdU Alexa Fluor 488 HCS Assay kit (Invitrogen), according to the instruction of the manufacturer.

Flow cytometric analysis

For flow cytometric analysis, cells were dissociated after the exposure to 0.2% EDTA for 20 min at room temperature. The cells in suspension were blocked with 1% BSA, incubated with specific primary antibodies, and then

stained with secondary antibodies. Negative control sample was incubated with a nonspecific antibody with the same isotype as the specific primary antibody, and stained with the same secondary antibody. 7-AAD (BD Pharmingen) was used to exclude dead cells. Cells were analyzed by using FACScan flow cytometer (Becton Dickinson) and FlowJo software (Tree Star).

RNA isolation for DNA microarray and qPCR

MVSCs derived from carotid arteries and jugular veins of SD rats were lysed with Trizol reagent (Invitrogen) and total RNA was extracted as previously described[42]. For microarray analysis, the RNA pellet was resuspended in nuclease-free H_2O and was subsequently diluted to a concentration of 0.50 mg/ml. Then, 10 µl of each sample was used for the analysis using an Affymetrix oligonucleotide microarray U133AA of Av2 chip containing 31,099 probe sets. Samples were labeled and hybridized according to Affymetrix protocols. Signal intensities were obtained for all probe sets and were organized using GeneTraffic version 3.2 microarray analysis software (Lobion). For qPCR, RNA pellets were resuspended in diethyl pyrocarbonate (DEPC)-treated H_2O. Complementary DNA was synthesized using two-step reverse transcription with the ThermoScript RT–PCR system (Invitrogen), followed by qPCR with SYBR green reagent and the ABI Prism 7,000 Sequence Detection System (Applied Biosystems). The sequences of the primers used in this study are shown in Table 2.1.

Table 2.1. Primer sequences

Gene	Forward	Reverse
Sox10	CTGGAGGTTGCTGAACGAGAGT	GTCCGGATGGTCTTTTTTGTG
Sox17	AGAACCCGGATCTGCACAAC	AGGATTTGCCTAGCATCTTGCT
Aggrecan	CTTCAAGCTGAACTATGACCACTTTACT	CATGGTCTGGAACTTCTTCTGAGA
SMA	TCCTGACCCTGAAGTATCCGATA	GGTGCCAGATCTTTTCCATGTC
CNN1	AGAACAAGCTGGCCCAGAAA	CACCCCTTCGATCCACTCTCT
18S	GCCGCTAGAGGTGAAATTCTTG	CATTCTTGGCAAATGCTTTCG

Tissue engineered nerve conduits with MVSCs and *in vivo* transplantation

Electrospinning technique was used to produce nerve conduits as previously described[20,24,42,43]. For cell transplantation into nerve conduits, MVSCs were isolated by using tissue explant culture method from the carotid arteries of transgenic GFP rats. The cell suspension was mixed with cold matrigel solution at a 2:1 ratio (volume to volume), and injected into the nerve conduits. The tissue-engineered constructs were kept in the incubator for 1 hour to allow gelation. The nerve conduit was inserted between the two nerve stumps and sutured, creating a gap of 1 cm between the two stumps.

Table 2.2 The marker expression in MVSCs

Antibody	MVSC	Company	Catalog #
SMA	low	Sigma	A2547
CNN1	-	Epitomics	1806-1
SM-22α	low	Abcam	Ab14106
NM-MHC	+	Abcam	Ab684
SM-MHC	-	Santa Cruz	sc6956
Myocardin	-	Santa Cruz	Sc-34238
Sox10	+	R&D	MAB2864
Slug	-	Santa Cruz	Sc-166476
Snail	+	Santa Cruz	Sc-28199
Pax-3/7	+	Santa Cruz	Sc-25409
Sox1	+	Chemicon	AB15766
Sox17	+	R&D	MAB1924
Nestin	+	Abcam	ab5968
AP-2α	-	DSHB	3b5
AP-2β	-	Santa Cruz	sc-6310
Vimentin	+	DAKO	M0725
Musashi	-	Chemicon	AB5977
p75	-	Abcam	ab8874
HNK1	-	Sigma	C-6680
NFM	+	Sigma	N4142
TUJ1	-	Chemicon	MAB1637
Peripherin	+	Chemicon	AB1530
Brn3a	+	Millipore	AB5945
Phox2b	+	Santa Cruz	Sc-13224
GFAP	-	DAKO	M0761

Carotid artery endothelial denudation model

The rat left common carotid arteries were subjected to endothelial denudation injury as described previously[44]. Briefly, adult SD rats were anesthetized with isoflurane. Endoluminal injury to the left common carotid artery was produced. Rats were sacrificed at 5, 15 and 30 days after injury, with at least 6 animals for each time point. The blood vessels samples were rinsed with PBS and embedded in OCT compound for histological analysis.

Staining and histological analysis

For immunostaining, cells or the tissue sections of blood vessels were fixed with 4% paraformaldehyde (PFA), permeabilized with 0.5% Triton X-100 (Sigma-Aldrich), and blocked with 1% BSA (Sigma-Aldrich). For actin cytoskeleton, samples were incubated with fluorescein isothiocyanate

Table 2.2 (Continued)

Antibody	MVSC	Company	Catalog #
S100β	+	Sigma	S2532
Oct4	-	Santa Cruz	Sc-5279
Nanog	-	Chemicon	AB9220
Sox2	-	Millipore	AB5603
Pax6	-	Covance	PRB-278P
O4	-	Millipore	MAB345
CD44	+	Biosource	AHS4411
CD29	+	Santa Cruz	Sc-9970
CD146	-	BD Phar	560846
PDX1	-	Millipore	AB3505
AFP	-	R&D	MAB-1368
CD133	-	Abcam	Ab19898
CD31	-	Chemicon	MAB1393
CD34	-	Sigma	M7786
C-kit	-	Abcam	Ab5506
Flk-1	-	BD Phar	555308
Sca-1	-	Abcam	ab51317
P63	-	Abcam	ab59691
CK14	-	Millipore	MAB3232
Alkaline phosphatase (ALP)	-	DSHB	B4-78
Collagen II	-	Chemicon	MAB8887
Sox9	-	Abcam	ab3697
CD14	-	Santa Cruz	Sc-1182

(FITC)-conjugated phalloidin (Invitrogen) for 30 min to stain filamentous actin (F-actin). For the staining of other cell markers, samples were incubated with specific primary antibodies (Table 2.2) for 2 hours at room temperature, washed with PBS for 3 times, and incubated with appropriate Alexa 488- and/or Alexa 546-labeled secondary antibodies (Invitrogen). Nuclei were stained with 4,6-diamidino-2-phenylindole (DAPI) (Invitrogen). Fluorescence images were collected by a Zeiss LSM710 confocal microscope. For organic dye staining, cells or the tissue sections were fixed with 4% PFA for 30 min, washed and stained with alizarin red (Sigma-Aldrich), alcian blue (Sigma-Aldrich), oil red (Sigma-Aldrich) or Verhoeff's dye (American MasterTech) according to the instruction of the manufacturers. Images were collected by a Zeiss Axioskop 2 plus microscope.

Statistics

Data were reported as means ± standard deviation (s.d.), unless otherwise indicated. All experiments were repeated at least three times. Comparisons among values for all groups were performed by one-way

analysis of variance (ANOVA). Holm's *t*-test was used for the analysis of differences between different groups. Significance level was set as $P < 0.05$.

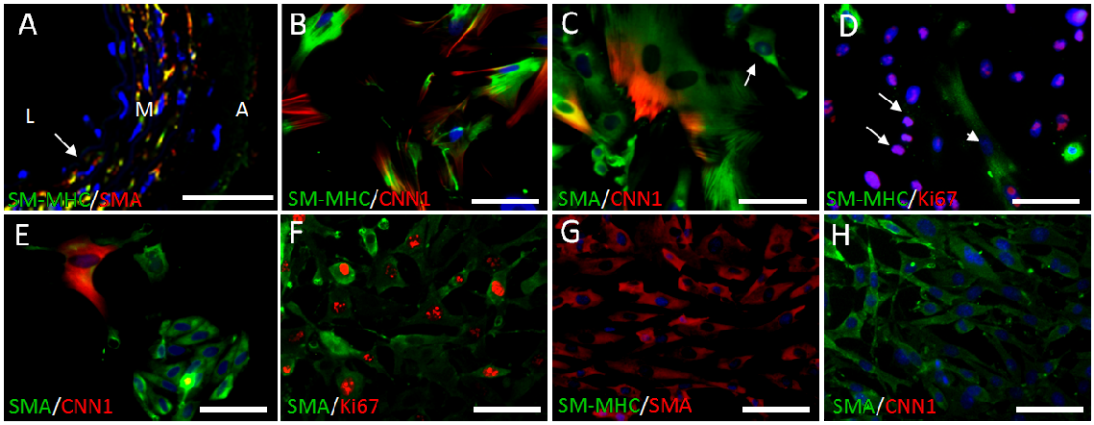

Figure 2.1. Identification of SM-MHC$^-$ cells in blood vessel. (A) Cross sections of carotid artery were stained for SM-MHC (red) and SMA (Green). Nuclei were stained with DAPI. L: lumen, M: media, A: adventitia. Arrow indicates a SM-MHC$^-$ cell inside tunica media. Scale bar is 50 μm. (B-E) Cells were isolated from arterial tunica media by using enzymatic digestion method. The derived cells were immunostained for SMA, SM-MHC, CNN1 and Ki67 after being cultured in DMEM with 10% FBS for 3 days. Arrow in C indicates a SM-MHC$^-$ cell. Arrows in D indicate proliferating SM-MHC$^-$ cells in culture. Arrowhead in D indicates a non-proliferative mature SMC. (F-H) Cells were isolated from arterial tunica media by using tissue explant culture method. The derived cells were immunostained for SMA, Ki67, SM-MHC and CNN1 after being cultured in DMEM with 10% FBS for 3 days. Scale bars are 100 μm.

2.3 Identification and characterization of rat MVSCs

First, we verified the existence of SM-MHC$^-$ cells in the tunica media by immunostaining the cross-sections of carotid arteries from SD rats for SMA and SM-MHC. As shown in Figure 2.1A, the majority of cells inside the elastic lamina layers were mature and contractile SMCs (SMA$^+$ /SM-MHC$^+$), whereas a small population (less than 10%) were negative for SM-MHC in the tunica media.

We then isolated and characterized the cells from the tunica media of carotid arteries of SD rats. Using enzymatic digestion, we obtained a mixed cell population including both mature SMCs and non-SMCs. The mature SMCs had SM-MHC and CNN1 assembled into stress fibers and were non-proliferative (negative for Ki67) (Figure 2.1B-D). By contrast, the SM-MHC$^-$ cells were smaller, had no SM-MHC, CNN1 or SMA in stress fibers, expressed low level of SMA, and were highly proliferative (Figure 2.1C, D). After being cultured in DMEM with 10% FBS for 3 days, the SM-MHC$^-$ cells started to multiply (Figure 2.1E) and eventually dominated the culture.

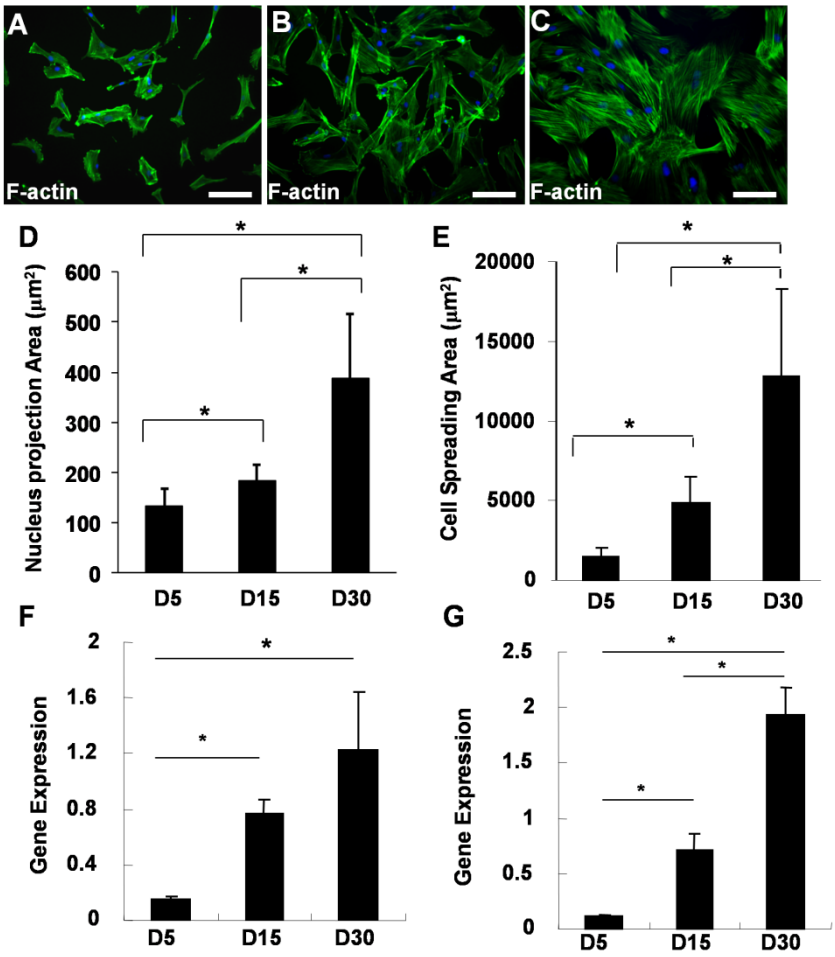

Figure 2.2. Characterization of SM-MHC$^-$ cells in culture. (A-C) SM-MHC$^-$ cells were cultured in DMEM with 10% FBS for 5, 15 and 30 days and were subjected to FITC-phalloidin staining for F-actin (Nuclei were stained with DAPI) (D, E) Quantification of nucleus projection area and cell spreading area during the spontaneous differentiation process of SM-MHC$^-$ cells isolated from carotid arteries and cultured for 5, 15 and 30 days in DMEM with 10% FBS. (F, G) qPCR was used to measure the gene expression of SMA and CNN1. 18S rRNA was used to normalize the relative expression levels. Data were shown as average ± s.d. (n=3). * indicates significant difference between indicated groups by using Holm's t-test (p<0.01).

With the tissue explant culture method, which relies on cell migration, only migratory and proliferative cells can be isolated. The cells migrating out of the tunica media expressed Ki67 and low levels of SMA, but did not express SM-MHC or CNN1 (Figure 2.1F-H). These cells had the same characteristics as the SM-MHC$^-$ cells isolated using the enzymatic digestion method. In the previous literature, these SM-MHC$^-$ cells were defined as synthetic and/or proliferative SMCs[45]. However, a detailed characterization showed that the SM-MHC$^-$ cells exhibited significant changes in morphology, during the culture for an extended period. The size of cell nucleus and the spreading area of the cells increased significantly (greater than threefold) within a 30-day time period, accompanied by the increase of stress fibers (Figure 2.2A-E) and the

increased expression of SMA and CNN1 (Figure 2.2F, G). These results suggest that the proliferative/synthetic SMCs might be derived from the spontaneous differentiation of SM-MHC$^-$ cells in the medium with 10% FBS.

To thoroughly characterize these SM-MHC$^-$ cells at the early stage (day 3) of primary tissue explant culture, we screened protein-marker expression with over 50 antibodies (Table 2.2), and found that isolated SM-MHC$^-$ cells uniformly expressed markers including neural crest cell markers Sox10, Sox1, Snail, vimentin and nestin, endoderm marker Sox17, neural cell makers NFM, peripherin, Brn3a, Phox2b and glial cell marker S100β (Figure 2.3A-H; Table 2.2), and general MSC makers including CD29 and CD44 (Figure 2.3I, J). In addition, these SM-MHC$^-$ cells were negative for CD146 and Sca-1 (Figure 2.3K, L), suggesting that these cells were distinct from previously identified perivascular MSC-like cell[46] or Sca-1$^+$ progenitors[47,48]. These cells were also negative for markers for EC and EC conversion-derived MSC-like cells, for example, CD31/PECAM1 and VE-cadherin[49], as well as the endothelial progenitor cell and HSC markers CD34, CD133, c-Kit and Flk-1 (Table 2.2).

To maintain the phenotype of these SM-MHC$^-$ cells, we performed screening for maintenance medium, and found a modified medium for neural crest stem cell (NCSC) culture that could maintain the cell morphology and the expression of aforementioned markers in the SM-MHC$^-$ cells. The maintenance medium contained DMEM with 2% CEE, 1% FBS, and 20 ng/ml of bFGF, and was used to expand the cells for further analysis.

We further determined whether they were capable of differentiating into ectodermal and mesodermal lineages by treating cells with specific differentiation induction media[15,24,47,50]. Indeed, these SM-MHC$^-$ cells were capable of differentiating into Schwann cell like cells (positive for glial fibrillary acidic protein, GFAP$^+$), peripheral neuron like cells (positive for neuron-specific class III β-tubulin, that is, TUJ1$^+$), SMCs (SM-MHC$^+$), chondrocytes (alcian blue staining), adipocytes (oil red staining) and osteoblasts (alizarin red staining) (Figure 2.4A-F).

The capability of the SM-MHC$^-$ cells differentiation into neural lineages was also demonstrated *in vivo*. We isolated SM-MHC$^-$ cells from tunica media of carotid arteries of transgenic GFP rats, and transplanted them into a nerve conduit to bridge transected sciatic nerve, as described[24]. After 1 month, immunostaining of the longitudinal-sections showed that GFP labeled cells differentiated into Schwann cells and contributed to axon myelination, as evident by myelin basic protein (MBP) expression (Figure 2.5).

These results indicate that these SM-MHC$^-$ cells in blood vessel wall are multipotent. Therefore, we defined these cells as MVSCs. MVSCs could be isolated from the tunica media of different blood vessels including jugular vein, aorta, abdominal artery, inferior vena cava, femoral artery and femoral vein beside carotid artery (Figure 2.6).

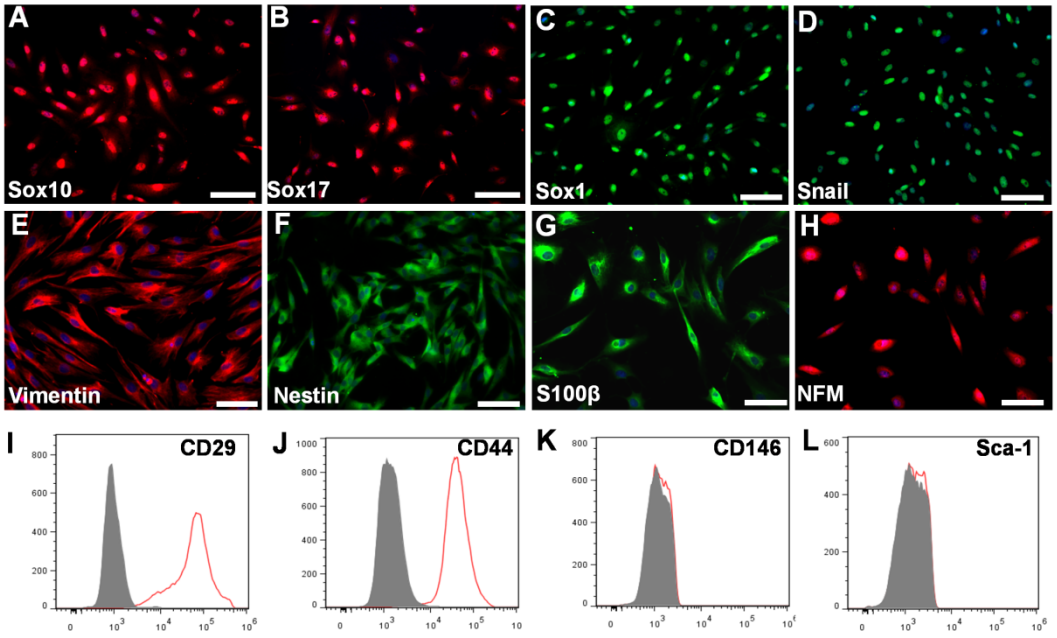

Figure 2.3. Characterization of SM-MHC$^-$ cells isolated from rat carotid arterial tunica media. (A-H) Immunostaining of isolated SM-MHC$^-$ cells cultured in DMEM with 10% FBS for 3 days for various markers, including Sox10, Sox17, Sox1, Snail, vimentin, nestin, S100β and NFM. (I-L) Flow cytometric analysis of SM-MHC$^-$ cells derived from arterial tunica media cultured in DMEM with 10% FBS for 3 days with antibodies against CD29, CD44, CD146 and Sca-1. Filled grey curves represent negative control samples, red curves represent samples stained with antibodies for CD29, CD44, CD146 or Sca-1. Scale bars are 100 μm.

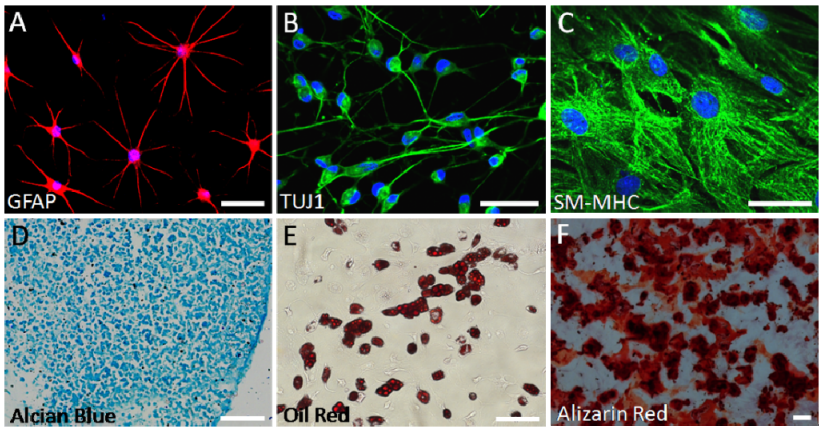

Figure 2.4. Multipotency of SM-MHC$^-$ cells. Staining of differentiated cell derived from SM-MHC$^-$ cells: Schwann cell like cells for GFAP (A), neuron like cells for TUJ1 (B), SMCs for SM-MHC (C), chondrocytes for aggrecan by using alcian blue (D), adipocytes for lipid droplets by using oil red (E) and osteoblasts for calcified matrix by using alizarin red (F). Scale bars of A-C are 50 μm. Scale bars of D-F are 100 μm.

2.4 Single-cell cloning and telomerase activity assay

To further confirm the stemness of MVSCs, we performed a cloning assay

(Figure 2.7A). Dilutional cell cloning assay showed that the average plating efficiency of MVSCs was about 13%, and the cloned MVSCs retained the marker expression, as described in Table 2.2, including Sox10, Sox17 (Figure 2.7B, C) and other MVSC markers (Data not shown), could self-renew and maintain the multipotency. To determine whether MVSCs had the capability to form neural spheres as neural crest cells[15,24,51], rat MVSCs derived from cloning assay were cultured on ultralow-attachment plates. Indeed, MVSCs formed neural sphere-like aggregates (Figure 2.7D), and the cells within the spheres retained the expression of the MVSC markers such as Sox17, vimentin, SMA, nestin and S100β (Figure 2.7E-I).

We then determined whether blood vessels and isolated MVSCs possess telomerase activity. Surprisingly, all blood vessels examined had telomerase activity, suggesting the presence of stem cells in the vascular wall (Figure 2.7J). The isolated MVSCs had a marked increase (>100 fold) of telomerase activity compared to the respective vascular tissues from which the cells were isolated, suggesting the enrichment and purification of stem cells from vascular tissues during the cell isolation process. Furthermore, we found no significant difference in telomerase activity in MVSCs isolated from different blood vessels.

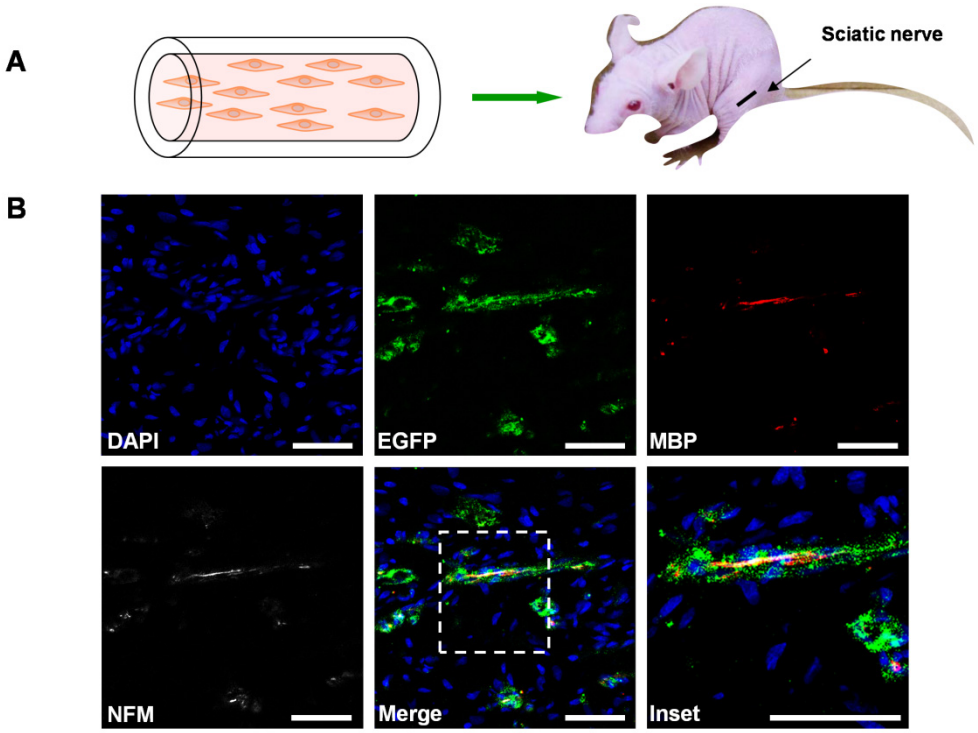

Figure 2.5. *In vivo* differentiation of MVSCs into Schwann Cells. (A) MVSCs isolated from transgenic GFP rats were embedded in matrigel inside the nerve conduit, and the nerve conduit was used to bridge the transected sciatic nerve in an athymic rat. (B) Staining of longitudinal-sections of a nerve conduit at 30 days after transplantation with antibodies against GFP, MBP and NFM. Nuclei were stained with DAPI. Scale bars are 50 μm.

We used carotid artery and jugular vein as representatives to further compare the MVSCs from different blood vessels. DNA microarray showed that MVSCs from carotid arteries and jugular veins were almost identical (Figure 2.7K), while only 3.6% of genes in expression showed significant difference of more than 2-fold, suggesting that MVSCs derived from arteries and veins were similar. DNA microarray also showed that MVSCs expressed MSC markers such as CD29, CD44, CD73 and CD90 (Data not shown).

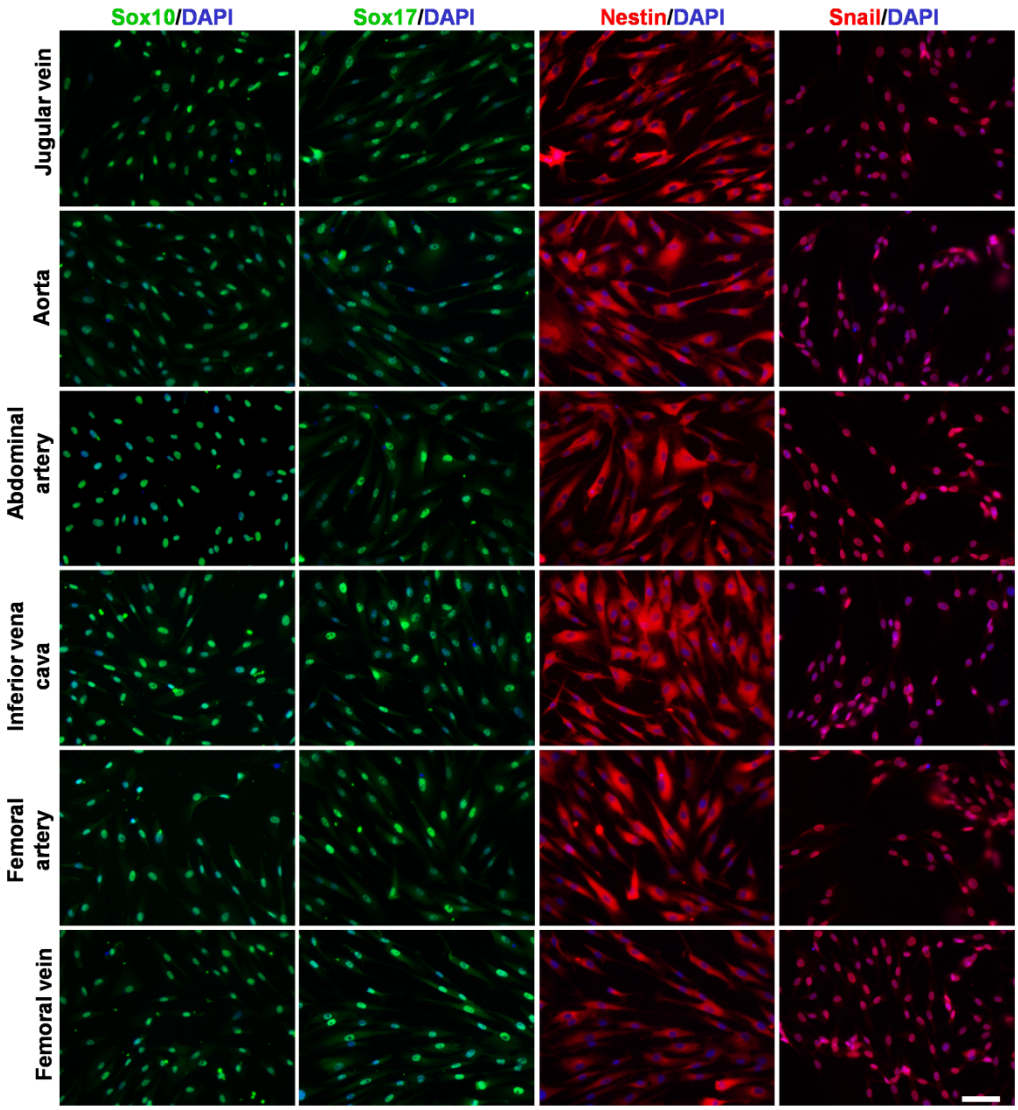

Figure 2.6. Characterization of MVSCs derived from different blood vessels in rats. Immunostaining of MVSCs derived from jugular vein, aorta, abdominal artery, inferior vena cava, femoral artery and femoral vein with antibodies against Sox10, Sox17, nestin and snail. Nuclei were stained with DAPI. Scale bar is 100 μm.

2.5 MVSC-MSC-SMC differentiation pathway

MVSCs could differentiate into SMCs, and the cells at various stages of differentiation could contribute to the heterogeneity of SMCs. It is also possible that previously identified MSC-like cells could be derived from MVSCs. Therefore, we examined the spontaneous differentiation of MVSCs by

culturing the freshly isolated MVSCs for 8 weeks in DMEM with 10% FBS. MVSCs were negative for CNN1 and SM-MHC (Figure 2.8A, D). After 3 weeks, MVSCs expressed CNN1 but lost the nuclear expression of Sox17

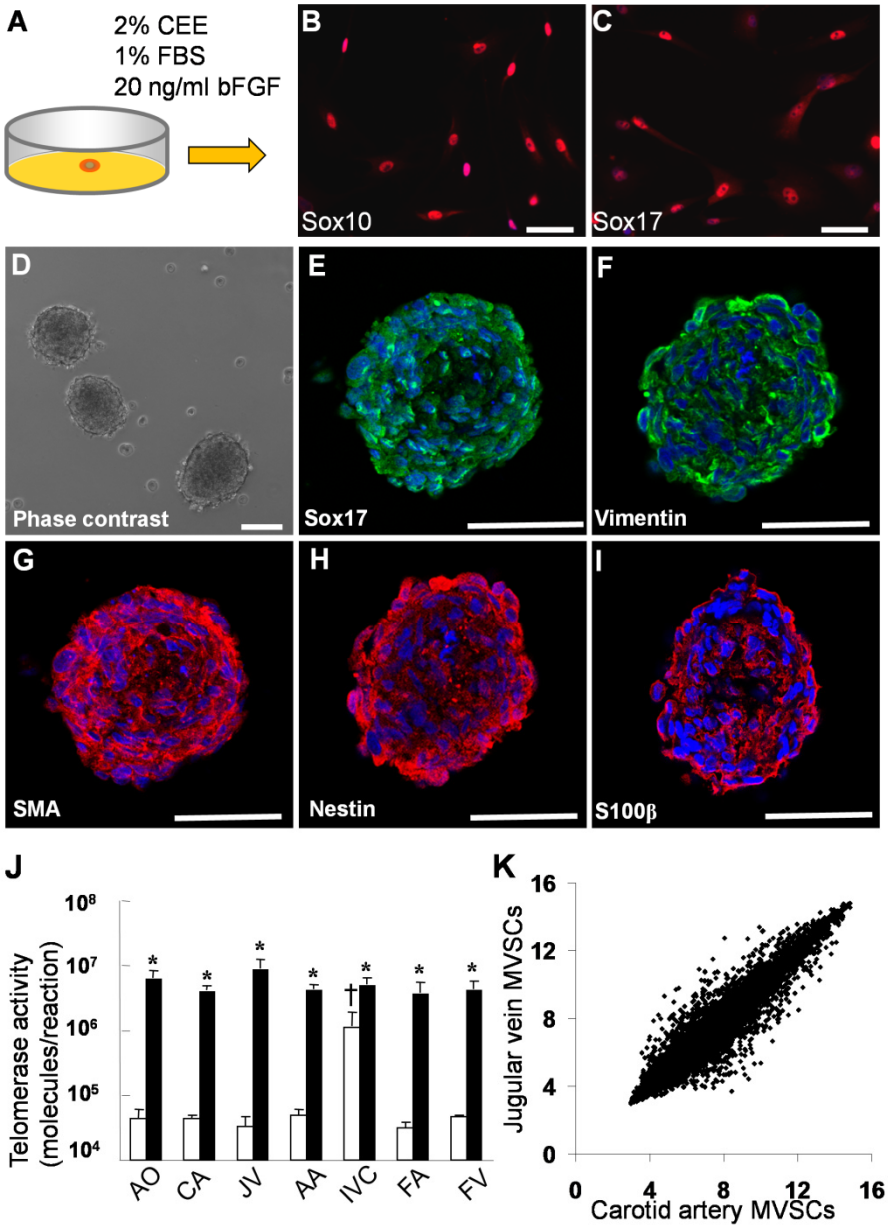

Figure 2.7. Single cell cloning of MVSCs. (A) Schematic illustration of single cell cloning with maintenance media. (B, C) Immunostaining of cloned MVSCs for Sox10 and Sox17. (D) Phase contrast image of neural spheres formed by cloned MVSCs. (E-I) Immunostaining of cross sections of neural spheres derived from MVSCs for MVSC markers including Sox17, vimentin, SMA, nestin and S100β. The nuclei were stained with DAPI. Scale bars are 50 μm. (J) Telomerase activity assay of MVSCs and the tissues from which MVSCs were isolated. The data was shown as average ± s.d. (n=3). White bars indicate tissues and black bars indicate isolated MVSCs. * indicates significant difference between MVSCs and the tissue from which the cells were derived by using Student's t-test (p<0.05). † indicates significant difference between inferior vena cava and other blood vessels (p<0.05). AO: aorta, CA: carotid artery, JV: jugular vein, AA:

abdominal artery, IVC: inferior vena cava, FA: femoral artery, FV: femoral vein. (K) DNA microarray analysis of MVSCs derived from rat carotid arteries and jugular veins (n=3).

($Sox17^-$ /$Sox10^+$ /$CNN1^+$ /SM-MHC^-) (Figure 2.8B, E). At this stage, the cells lost the capability of differentiating into peripheral neurons and Schwann cells, but retained the potential for SMC, osteogenic, chondrogenic and adipogenic differentiation (summarized in Figure 2.8G), similar to previously reported MSC-like cells. These results suggested that MVSCs could be the precursor of MSC-like cells identified in blood vessel by previous studies [15,52,53].

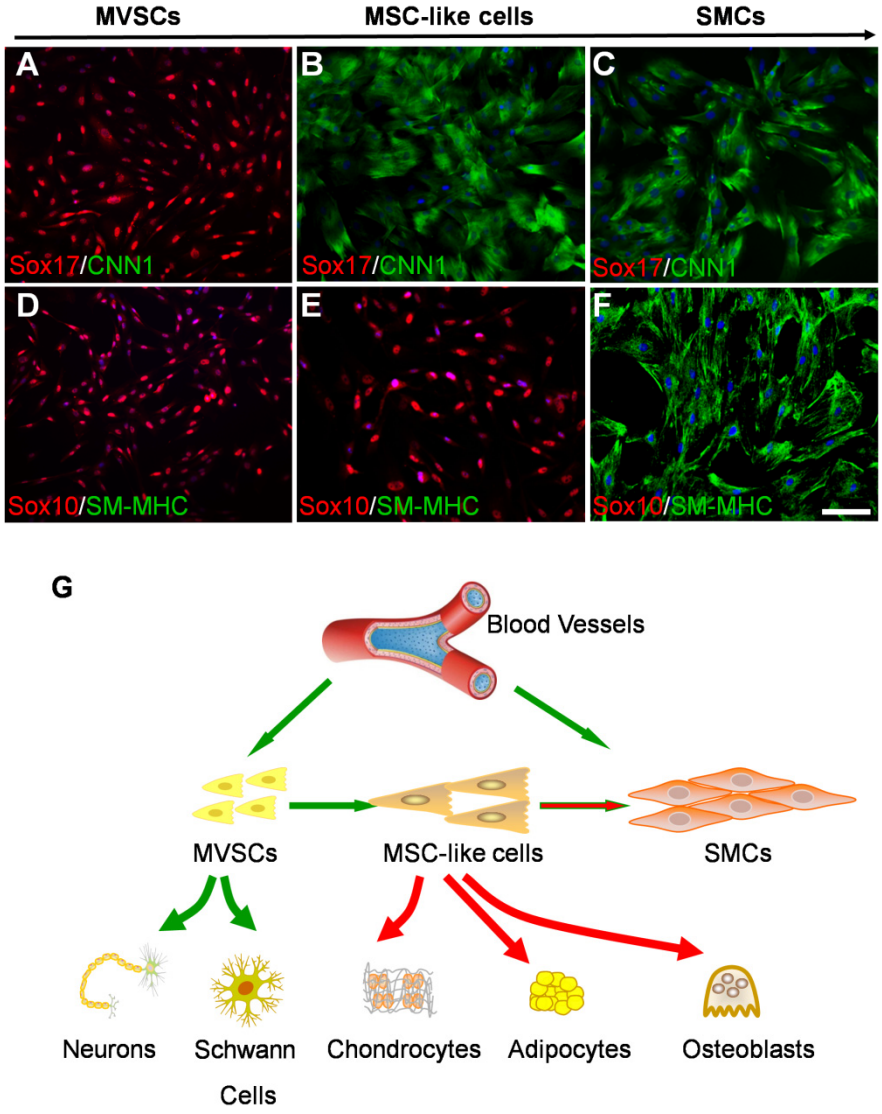

Figure 2.8. Spontaneous differentiation of MVSCs into MSC-like cells and SMCs. (A-F) MVSCs were cultured in DMEM with 10% FBS for 5 (A, D), 3 weeks (B, E) and 8 weeks (C, F), and were immunostained for Sox17, CNN1, SM-MHC and Sox10. Scale bar is 100 μm. The nuclei were stained with DAPI. (G) Schematic illustration of the spontaneous differentiation of MVSCs and the differentiation potential of the cells at different stages.

In addition, after being cultured in DMEM with 10% FBS for 8 weeks, the

cells lost the expression of Sox17 and Sox10 and spontaneously differentiated into mature SMCs ($CNN1^+$/$SM\text{-}MHC^+$) (Figure 2.8C, F). These cells also lost the differentiation potential into neural and mesenchymal lineages

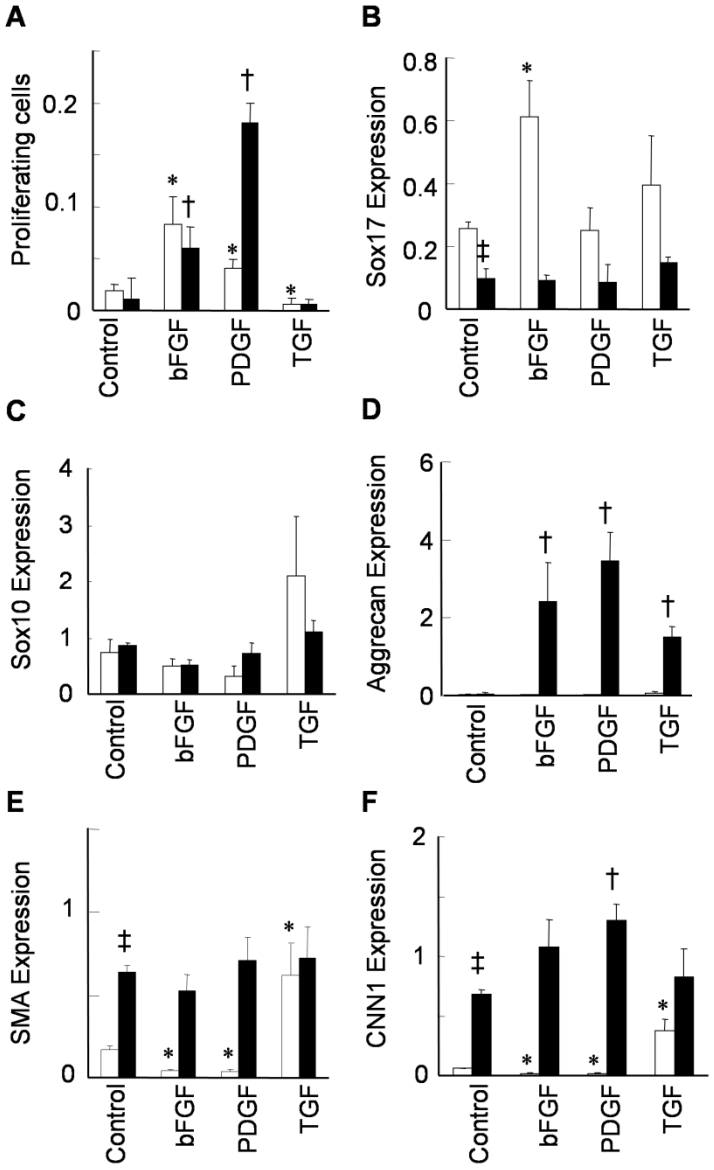

Figure 2.9 Differential responses of MVSCs and MSC-like cells to the treatment of vascular growth factors. The undifferentiated MVSCs and MSC-like cells (cultured in DMEM with 10% FBS for 3 weeks) were treated with 10 ng/ml bFGF, 10 ng/ml PDGF-B or 10ng/ml TGF-β1 for 24 hours. White bars indicate undifferentiated MVSCs and black bars indicate MSC-like cells. (A) EdU staining was used to quantify the proliferating cells. (B-F) qPCR analysis was used to quantify the gene expression of Sox17 (B), Sox10 (C), aggrecan (D), SMA (E) and CNN1 (F). 18S rRNA was used to normalize the relative expression levels. Data were shown as average ± s.d. (n=3). * indicates significant difference between growth factors-treated and untreated MVSCs (p<0.05). † indicates significant difference between growth factor-treated and untreated MSC-like cells (p<0.05). ‡ indicates significant difference between MVSCs and MSC-like cells in absence of growth factors (p<0.05).

(Summarized in Figure 2.8G). These results suggested that long-term culture in the medium containing 10% FBS resulted in the spontaneous differentiation of MVSCs into MSC-like cells and subsequently SMCs and that the cells at the various stages of differentiation might explain the heterogeneity of SMCs.

2.6 Differential response of MVSCs and differentiated cells

MVSCs at different stages of differentiation might respond differently to the same stimulation in the vascular microenvironment. To address this issue, we compared the effects of three vascular growth factors on undifferentiated MVSCs and MSC-like cells (3-week differentiation) as an example. The vascular growth factors used in this study included bFGF, PDGF-B and TGF-β1. PDGF-B and bFGF increased the proliferation of both MVSCs and MSC-like cells, while TGF-β1 suppressed the proliferation of MVSCs (Figure 2.9A). It was also noted that PDGF-B had more dramatic effect on the proliferation of MSC-like cells compared with MVSCs.

qPCR showed that MSC-like cells had much lower expression of MVSC marker such as Sox17 and higher expression of early SMC markers such as SMA and CNN1 (Figure 2.9B, E, F). bFGF significantly increased Sox17 expression while suppressed the expression of SMC markers including SMA and CNN1 of MVSCs (Figure 2.9B, E, F), suggesting that bFGF might help maintain MVSCs at undifferentiated state. However, bFGF had no significant effect on the expression of Sox17, SMA and CNN1 but increased the synthesis of aggrecan (Figure 2.9D) in MSC-like cells, suggesting that bFGF might promote a synthetic SMC phenotype in MSC-like cells.

PDGF-B also suppressed the expression of SMC markers of MVSCs (Figure 2.9E, F), but did not show any effect on Sox17 expression (Figure 2.9D). In MSC-like cells, PDGF increased aggrecan synthesis and CNN1 expression, but had no effect on the expression of SMA (Figure 2.9D-F).

TGF-β1 significantly increased the expression of early SMC markers including SMA and CNN1 of MVSCs (Figure 2.9E, F), suggesting that TGF-β1 promoted MVSC differentiation into SMC lineage. In MSC-like cells, TGF-β1 promoted synthetic SMC phenotype by increasing the synthesis of aggrecan (Figure 2.9D), similar to bFGF and PDGF. These results demonstrated the MVSCs and differentiated cells responded differently to vascular growth factors.

2.7 MVSC activation *in vitro* and *in vivo*

Cell proliferation and expansion are important in the development of vascular diseases. Therefore, we performed *in vitro* and *in vivo* studies to determine the transition of MVSCs from quiescent state to proliferative state. We first isolated MVSCs from carotid arteries of SD rats by using enzymatic digestion method. Within 24 hours after cell isolation, immunostaining showed that MVSCs only expressed low levels of SMA, but not Sox10 or Ki67 (Figure

2.10A, B), which indicated that MVSCs were quiescent in the blood vessels. However, after being cultured for another 24 hours, MVSCs started expressing Sox10, nestin as well as Ki67 (Figure 2.10C-F), suggesting that MVSCs were activated and became proliferative.

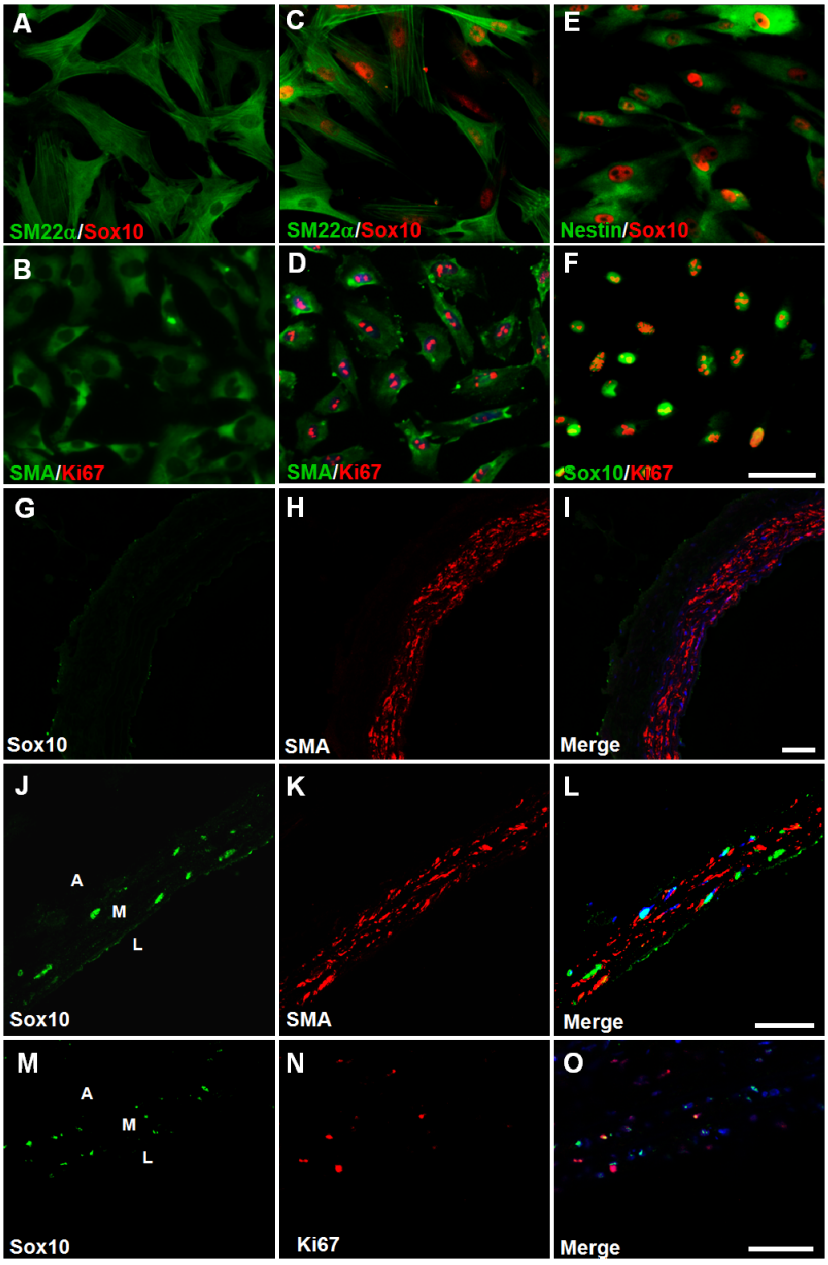

Figure 2.10. MVSC activation *in vitro* and *in vivo*. MVSCs were isolated from rat carotid arteries by using enzymatic digestion method, and cultured in DMEM with 10% FBS for 24 hours (A, B) and 48 hours (C-F). The cells were immunostained for SMA, SM22α, Nestin, Ki67 and Sox10. Scale bar is 100 μm. (G-O) Immunostaining of cross sections from native carotid arteries (G-I) and injured carotid arteries (day 5) (J-O) with the antibodies against Sox10, SMA, Ki67, S100β and NFM. A: Adventitia, L: Lumen, M: Media. The nuclei were stained with DAPI. Scale bars are 50 μm.

Immunostaining also confirmed that the cells in the normal blood vessel

wall did not express detectable level of MVSC markers (e.g., Sox10) or proliferation marker Ki67 (Figure 2.10G-I), suggesting that MVSCs were quiescent under normal physiological conditions. Upon vascular endothelial denudation injury[44], about 50% of cells inside the elastic lamina layers of arterial media were found expressing Sox10 at day 5 after injury (Figure 2.10J-L), and about 40% of $Sox10^+$ cells were positive for proliferative marker Ki67 (Figure 2.10M-O). The percentage of proliferating cells is similar to what has been reported in the previous publications[54,55,56]. The $Ki67^+$ cells were found only in $Sox10^+$ MVSC population in tunica media, further confirming that MVSCs instead of SMCs could be activated to enter cell cycle upon vascular injury. Of note, we also found Ki67-expressing cells in endothelial layer and adventitia layer after injury, indicating that endothelial cells and adventitial cells were also activated to enter cell cycle for vascular remodeling.

*2.*8 Conclusion

In summary, we identify a new type of multipotent vascular stem cell in blood vessel wall. MVSCs express markers including Sox17, Sox10 and S100β, are cloneable, have telomerase activity, and can differentiate into neural lineages and MSC-like cells that subsequently differentiate into SMCs. In addition, we found that the MVSCs at different stages respond differently to various stimuli like the vascular growth factors. There are currently over 40,000 papers on SMC biology. Our data provide new explanation for the controversial conclusions in this field. Many of the previous data explanation and interpretations should be revisited. Furthermore, MVSCs are dormant in native tissues. Upon vascular injury, the cells can be activated and rapidly expanded to contribute to vascular remodeling.

Chapter 3. Differentiation of MVSCs Contributes to Vascular Diseases

3.1 Motivation

In Chapter 2, we identified MVSCs, which express markers including Sox17, Sox10 and S100β, are cloneable, have telomerase activity, and can differentiate into neural cells and MSC-like cells that subsequently differentiate into SMCs. Moreover, previously identified synthetic/proliferative SMCs are likely derived from the differentiation of MVSCs. Therefore, the next question is whether MVSCs are derived from de-differentiation of contractile SMCs.

To date, SM-MHC is generally deemed as the most specific marker of mature and contractile SMCs[57]. Therefore, we utilized SM-MHC-Cre mice, originally made by Michael Kotlikoff's lab[58] using a SM-MHC promoter-enhancer provided by Owens Lab, which faithfully recapitulates expression of endogenous SM-MHC gene [59]. The SM-MHC-Cre mice were crossed with a Cre activatable indicator mouse strain, ROSA26-loxP-EGFP, obtained from Jackson labs. The progeny having both the two constructs were used in the following study.

3.2 Methods and materials

Generation of transgenic mice and genotyping

Animal studies were approved by the ACUC committee at UC Berkeley, and were carried out according to the institutional guidelines. Transgenic mice, expressing Cre recombinase under the control of the SM-MHC promoter were mated with transgenic mice with a construct of Rosa26-loxP-EGFP or Actin-loxP-EGFP (Jackson laboratory, Inc.) to generate SM-MHC-Cre/loxP-EGFP mice. The sequences of primers used for genotyping were shown in Table 3.1.

Table 3.1. Primer sequences used for genotyping.

Transgene	Forward	Reverse
SM-MHC-Cre	GCGGTCTGGCAGTAAAAACTATC	GTGAAACAGCATTGCTGTCACTT
Rosa26-loxP-lacZ	AAAGTCGCTCTGAGTTGTTAT	GCGAAGAGTTTGTCCTCAACC
Rosa26-loxP-EGFP	GAGTTCTCTGCTGCCTCCTG	AAGACCGCGAAGAGTTTGTC
β-actin-LoxP-EGFP	AAGTTCATCTGCACCACCG	TCCTTGAAGAAGATGGTGCG

Cell isolation

Cells were isolated from the blood vessels of SM-MHC-Cre/loxP-EGFP. The cells isolation methods were described previously[40]. Briefly, the tissue

segments were washed three times with PBS supplemented with 1% P/S. The surrounding connective tissues and adventitia were dissected away under a dissecting microscope. Endothelium was removed by scraping off the cell layer on the luminal surface with sterile scalpel blades. For tissue explant culture method, the tunica media was cut into mm-size and placed onto the surface coated with 1% CellStart in 6-well plates. The cells were cultured in DMEM with 10% FBS, or in DMEM with 2% CEE, 1% FBS, 1% N2, 2% B27, 100 nM RA, 50 nM 2ME, 1% P/S and 20 ng/ml bFGF. For enzymatic digestion methods, tissues were incubated with 3 mg/ml type II collagenase in DMEM with a 1/5 (w/v) ratio of tissue (g) to enzyme solution (ml). After incubation at 37°C for 30 min, the same volume of 1 mg/ml elastase solution was added to the solution containing the tissue and collagenase. The tissues were incubated for another 1-2 hours until all the tissues were digested. Cells were then seeded onto CellStart-coated dishes and maintained at 37°C in an incubator with 5% CO_2. For the directed differentiation of MVSCs into peripheral neurons, Schwann cells, osteoblasts, adipocytes and chondrocytes, the cells were incubated in specific induction media described previously for 1-3 weeks [24,41].

Carotid artery endothelial denudation model

The SM-MHC-Cre/loxP-EGFP mouse carotid arteries were subjected to endothelial denudation injury as described previously [44]. Briefly, transgenic mice were anesthetized with isoflurane. Endoluminal injury to the left common carotid artery was produced. Mice were sacrificed at 5, 15 and 30 days after injury, with at least 6 animals for each time point. The blood vessels samples were rinsed with PBS and embedded in OCT compound for histological analysis.

***In vivo* transplantation**

For the transplantation of MVSCs into microfibrous vascular grafts[60], MVSCs were derived from the carotid arteries of SM-MHC-Cre/loxP-EGFP mice by using the tissue explant culture method. MVSCs were mixed with neutralized collagen solution (2 mg/ml; diluted in MVSC maintenance medium), resulting a cell density at 1 million cells/0.5 ml. The collagen gel solution (with cells) was then used to fill in the space outside of the vascular graft in a 1-ml syringe and allowed to polymerize at 37ºC for 1 hour. Then DMEM with 10% FBS containing 10 ng/ml TGF-β1 was added into the syringe to cover the grafts. After 1-day culture, the gel was contracted by the embedded cells and attached tightly onto the outer surface of the graft. The vascular grafts with cells were then transplanted into athymic rats by using carotid artery anastomosis.

Staining and histological analysis

For immunostaining, cells or the tissue sections of blood vessels were

fixed with 4% PFA, permeabilized with 0.5% Triton X-100, and blocked with 1% BSA. Samples were incubated with specific primary antibodies (Table 2.1) for 2 hours at room temperature, washed with PBS for 3 times, and incubated with appropriate Alexa 488- and/or Alexa 546-labeled secondary antibodies. Nuclei were stained with DAPI. Fluorescence images were collected by a Zeiss LSM710 confocal microscope.

For organic dye staining, cells or the tissue sections were fixed with 4% PFA for 30 min, washed and stained with alizarin red, alcian blue, oil red or Verhoeff's dye according to the instruction of the manufacturers. Images were collected by a Zeiss Axioskop 2 plus microscope.

Flow cytometric analysis

For flow cytometric analysis, cells were dissociated after the exposure to 0.2% EDTA for 20 min at room temperature. The cells in suspension were blocked with 1% BSA, and subjected to EGFP detection. 7-AAD was used to exclude dead cells. Cells were analyzed by using FACScan flow cytometer and FlowJo software.

3.3 MVSCs did not arise from the de-differentiation of contractile SMCs

Our results suggest that previously identified proliferative or synthetic SMCs could be MVSCs and/or their derivatives following spontaneous differentiation in regular culture media. To directly determine whether MVSCs are derived from the de-differentiation of contractile SMCs, we performed lineage tracing by using SM-MHC as a marker in the SM-MHC-Cre/loxP-EGFP mice[57,58,61]. Immunostaining showed that less than 10% of the cells in the carotid arterial tunica media of SM-MHC-Cre/loxP-EGFP mice were not labeled with EGFP, indicating the existence of a small population of non-SMCs in the tunica media (Figure 3.1A), consistent with the observation in the rat model. Immunostaining for Cre and EGFP further showed that the $EGFP^-$ cells did not express Cre (Data now shown).

With enzymatic digestion culture, majority (about 92%) of the cells isolated from the carotid arteries of SM-MHC-Cre/loxP-EGFP mice were $EGFP^+$ cells (Figure 3.1B). However, after being cultured and passaged in DMEM with 10% FBS for 10 days, all the cells in culture were $EGFP^-$ (Figure 3.1C), indicating that these cells were not derived from contractile SMCs. In addition, in tissue explant culture, migratory and proliferative cells were $EGFP^-$ in contrast to strong EGFP fluorescence in the arterial tunica media (Figure 3.1D, E). Flow cytometry also confirmed that none of the derived vascular cells expressed EGFP, which indicated that proliferative and migratory cells isolated from tunica media of blood vessels were not derived from the de-differentiation of contractile SMCs (Figure 3.1F). The lack of EGFP expression in MVSCs was unlikely due to the suppression of Rosa26 promoter activity in cell culture[62]. When SM-MHC-Cre/loxP-EGFP mice were generated by using β-actin (instead of ROSA26) promoter to drive the EGFP expression, tissue

explant culture showed that cells derived from these mice did not express EGFP, while vascular cells in the tissue explant expressed EGFP (Fig. 3.2).

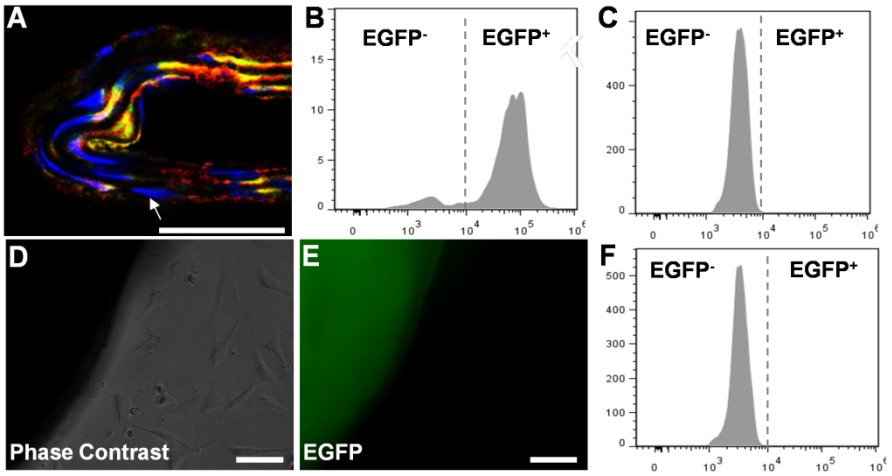

Figure 3.1. MVSCs did not arise from mature SMCs. (A) A cross-section of carotid artery from SM-MHC-Cre/loxP-EGFP mouse was immunostained for EGFP (green) and SMA (red). The arrow indicates a SM-MHC$^-$ cell inside tunica media. Scale bar is 50 μm. (B, C) Flow cytometric analysis for EGFP of cells derived from carotid arteries of SM-MHC-Cre/loxP-EGFP mice by using enzymatic digestion method at day 0 (B) (n=3) and day 10 (C) (n=3), with the cells cultured in DMEM with 10% FBS. (D, E) Phase contrast and fluorescent images of tissue explant culture of carotid arterial tissue from SM-MHC-Cre/loxP-EGFP mice. Scale bars are 100 μm. (F) Flow cytometric analysis for EGFP expression in the cells derived in D and E (n=6).

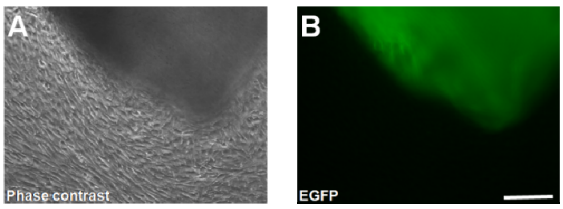

Figure 3.2. MVSC isolation from lineage tracing mice with β-actin promoter. MVSCs were derived from the carotid arteries of SM-MHC-Cre/Actin-loxP-EGFP mice by using tissue explant culture method. (A) Phase contrast image of MVSCs and the tissue chunk from which the cells migrated from. (B) FITC channel was used to detect the EGFP signal. Scale bar is 100 μm.

To determine whether these EGFP$^-$ cells were similar to rat MVSCs, immunostaining and differentiation assay were performed. Immunostaining showed that these EGFP$^-$ cells uniformly expressed the same MVSC markers including Sox10, Sox17, Sox1, Snail, S100β and NFM (Figure 3.3). In addition, these cells could be induced to differentiate into Schwann cell like cells (GFAP$^+$/S100β$^+$), peripheral neuron like cells (TUJ1$^+$/peripherin$^+$), chondrocytes (alcian blue$^+$), adipocytes (oil red$^+$) and osteoblasts (alizarin red$^+$)

(Figure 3.4 A-E), which further confirmed that EGFP$^-$ cells in tunica media were MVSCs.

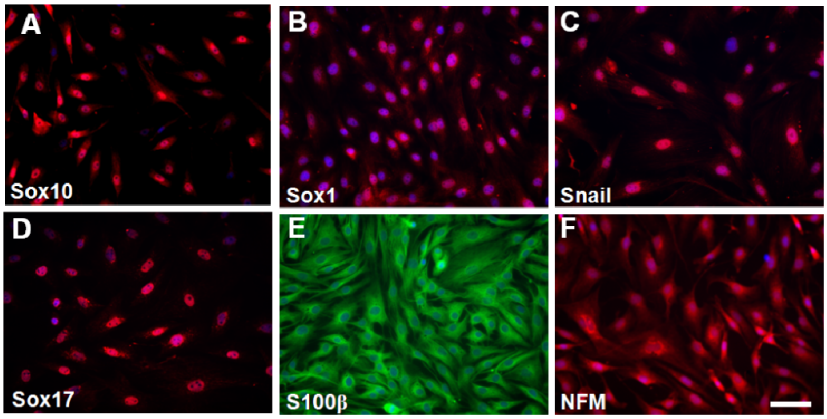

Figure 3.3. Marker expressions of EGFP$^-$ cells. Staining of EGFP$^-$ cells with antibodies against Sox10, Sox1, snail, Sox17, S100β and NFM. Scale bar is 100 μm.

3.4 Differentiation into mature SMCs *in vitro* and *in vivo*

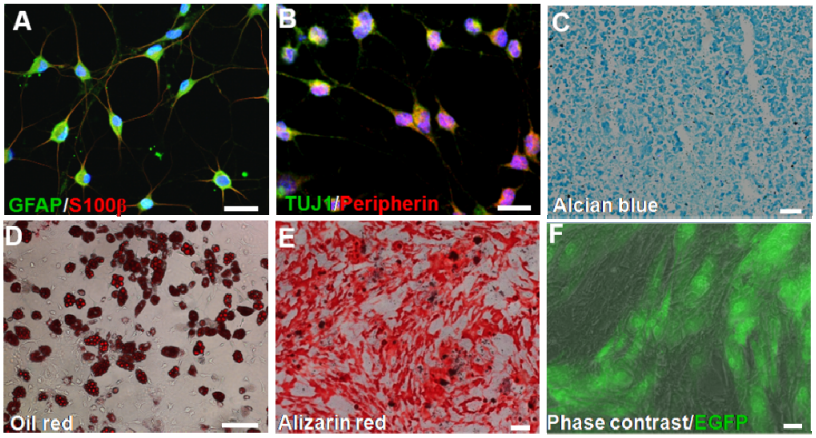

Figure 3.4. Multipotency of EGFP$^-$ cells. Staining of differentiated cells derived from EGFP$^-$ cells: Schwann cell like cells for GFAP and S100β (A), neuron like cells for TUJ1 and peripherin (B), chondrocytes for aggrecan by using alcian blue (C), adipocytes for lipid droplets by using oil red (D) and osteoblasts for calcified matrix by using alizarin red (E). Scale bars in A and B are 50 μm. Scale bars of C-E are 100 μm. (F) EGFP expression in MVSCs after being co-cultured with OP9-Delta1 cell line for 2 weeks. Scale bar is 50 μm.

To determine whether MVSCs could differentiate into mature SMCs and turn on EGFP expression, we activated Notch signaling by co-culturing EGFP$^-$ MVSCs with OP9-Delta1 feeder cells [63]. After two weeks of co-culture, majority of the MVSCs showed strong green fluorescence (Figure 3.4F). Immunostaining for SM-MHC confirmed that MVSCs indeed differentiated into SM-MHC$^+$ SMCs (Figure 3.5A-C). The fact that EGFP could be turned on after MVSCs differentiated into SMCs further confirmed that MVSCs are not derived

from de-differentiation of contractile SMCs. Interestingly, a small portion of the EGFP$^+$ cells expressed proliferation marker Ki67 (Figure 3.5D-F), suggesting that newly differentiated SMCs had not exit cell cycle yet.

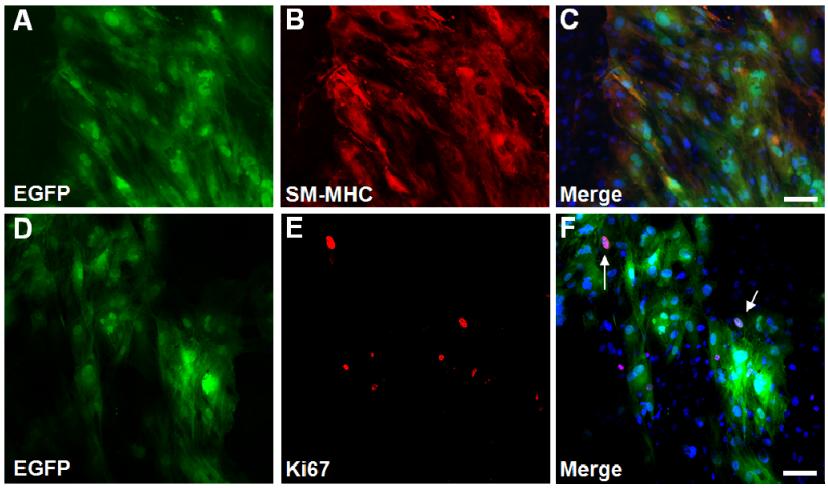

Figure 3.5. EGFP expression after MVSCs differentiated into SMCs. EGFP$^-$ cells were derived from SM-MHC-Cre/loxP-EGFP mice, co-cultured with OP9-Delta1 feeder cells for 2 weeks, and became EGFP$^+$ cells. (A-C) EGFP$^+$ cells were immunostained with an antibody against SM-MHC. (D-F) EGFP$^+$ cells were immunostained with an antibody against Ki67. Arrows indicate proliferating EGFP$^+$ cells. Nuclei were stained with DAPI. Scale bars are 100 μm.

To test whether MVSCs could differentiate into mature SMCs and turn on EGFP expression *in vivo*, we embedded MVSCs in collagen gel on the outer surface of a nanofibrous vascular graft, and implanted the grafts into athymic rats by performing carotid artery anastomosis [20,42]. After 1 month, immunostaining of the cross-sections showed that a small portion of the cells expressed EGFP, suggesting that MVSCs could differentiate into mature SMCs *in vivo* (Figure 3.6).

3.5 MVSCs contribute to vascular remodeling

To further investigate the fate of SMCs after vascular injury, we performed endothelial denudation injury in the carotid artery of SM-MHC-Cre/loxP-EGFP mice. Immunostaining showed that the cells in native carotid artery express EGFP but not MVSC marker S100β (Figure 3.7A-C).

Surprisingly, at day 5 after injury, the majority of the cells in tunica media expressed S100β instead of EGFP (Figure 3.7D-F), which is consistent with previous notion that most SMCs may die by apoptosis while remaining cells proliferate and repopulate tunica media after vascular injury [64,65]. Although a low number of EGFP$^+$ cells were found at this time point, none of them expressed proliferation marker Ki67 (Data not shown). Thus, MVSCs were activated and proliferated rapidly to repopulate the tunica media after injury and contributed to vascular remodeling.

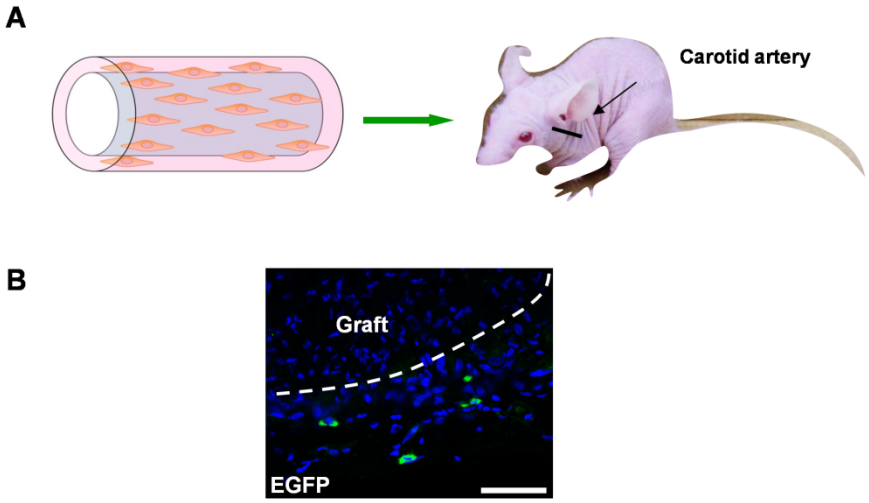

Figure 3.6. *In vivo* differentiation of MVSCs into SMCs. (A) MVSCs derived from SM-MHC-Cre/loxP-EGFP mice were embedded in collagen gel on the outer surface of a nanofibrous PLLA vascular graft. The construct was transplanted into an athymic rat by performing carotid artery anastomosis. (B) Staining of cross-sections of a vascular graft with an antibody against EGFP at 1 month after transplantation. Nuclei were stained with DAPI. Scale bar is 50 μm. Dashed line indicates the boundary of the graft and collagen gel. $EGFP^+$ cells indicate the differentiation of MVSCs into SM-MHC expressing SMCs.

The neointima formation was observed around day 15 after endothelial denudation injury in rat carotid arteries. Majority of the cells in the tunica media and neointima expressed MVSC makers including Sox10 at day 15 and 30 (Figure 3.8G-I), indicating that MVSCs were the major cell type in tunica media and neointima after vascular remodeling. Immunostaining also confirmed that the cells in neointima expressed other MVSC markers such as NFM and S100β(Figure 3.7J-L). At 30 days after injury, majority of the cells started to express SM-MHC (Figure 3.7M-O) and some of the cells were still proliferating (Data not shown), which is consistent with the *in vitro* observation that the newly differentiated SM-MHC^+ cells might have not exit cell cycle yet.

3.6 MVSCs contribute to blood vessel calcification

At 1 month post injury, Verhoeff's staining and alcian blue staining showed significant deposition of aggrecan and collagen I respectively in neointima populated by MVSCs (Figure 3.8A and Figure 3.9A), suggesting that MVSCs-derived cells had synthetic phenotype and contributed to the matrix synthesis during neointima formation. Immunostaining showed that some of the MVSCs in neointima differentiated into chondrogenic cells ($S100\beta^+$/collagen II^+) (Figure 3.8B), which demonstrated a novel mechanism

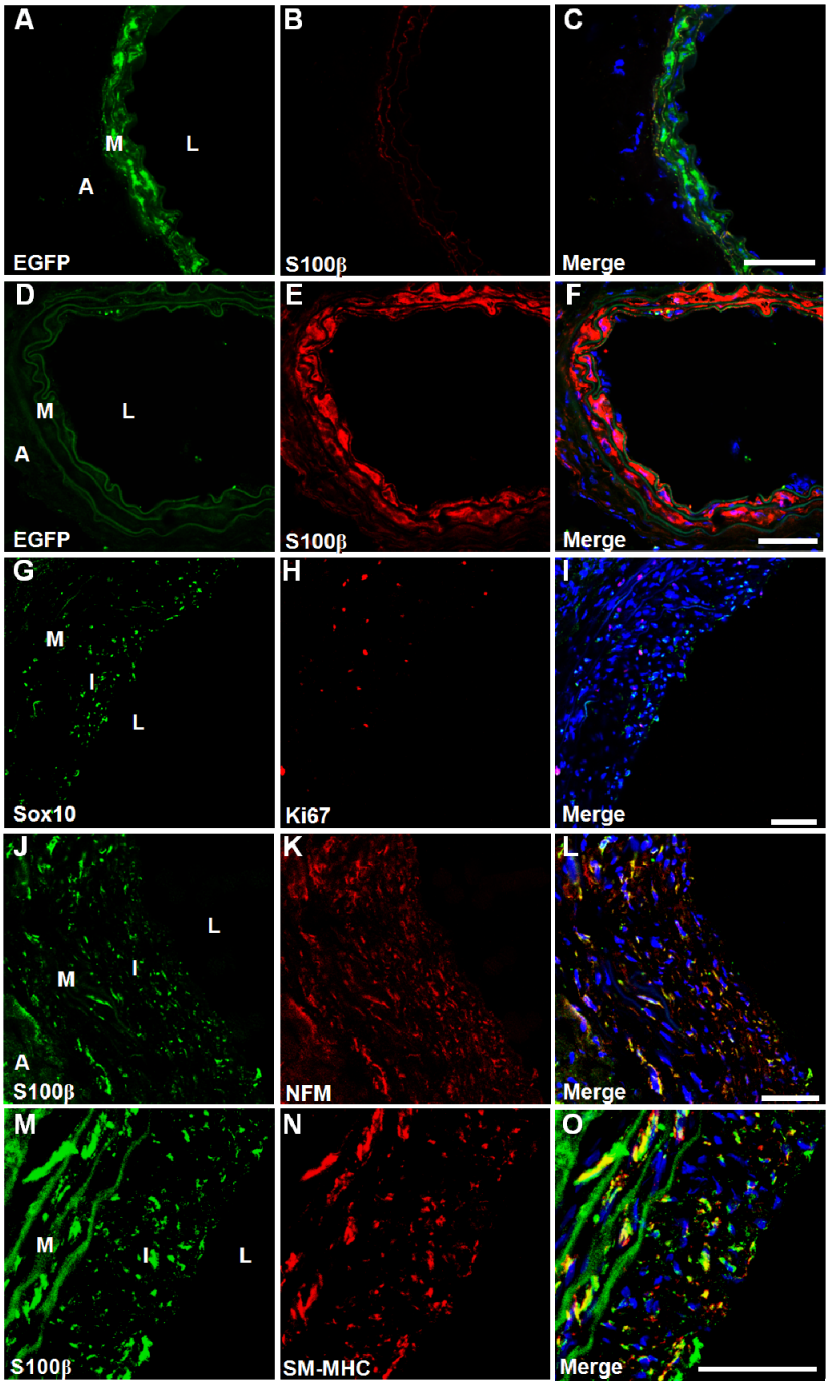

Figure 3.7. MVSCs contributed to vascular remodeling and neointima formation after vascular injury. (A-F) Immunostaining of cross-sections of native carotid arteries (A-C) and injured carotid arteries (day 5) (D-F) from SM-MHC-Cre/loxP-EGFP mice with the antibodies against EGFP and S100β. (G-I) Immunostaining of cross-sections from carotid arteries of SD rats at day 15 after injury with the antibodies against Sox10, Ki67, S100β and NFM. (M-O) Immunostaining of cross sections of carotid arteries from SD rats at day 30 after injury with the antibodies against S100β and SM-MHC. Scale bars are 50 μm. The nuclei were stained with DAPI. A: adventitia, I: intima, L: lumen, M: media.

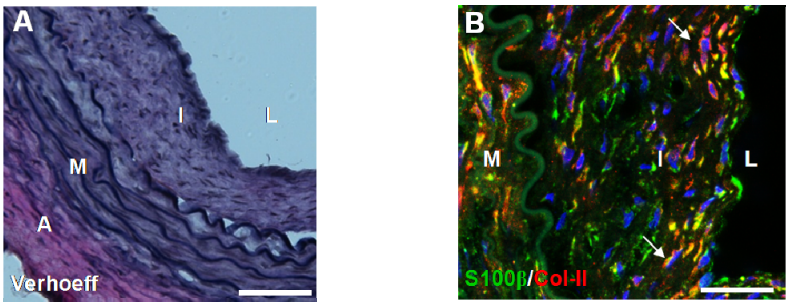

Figure 3.8. Matrix synthesis by MVSCs in neointima. (A) A cross-section of carotid artery at 5 weeks after injury was subjected to Verhoeff's staining. (B) Immunostaining of a cross-section of injured carotid artery with antibodies against S100β (green) and collagen II (red). Arrows indicate cells expressing both S100β and collagen II. A: adventitia. M: media. I: intima. L: lumen. Scale bars are 50 μm.

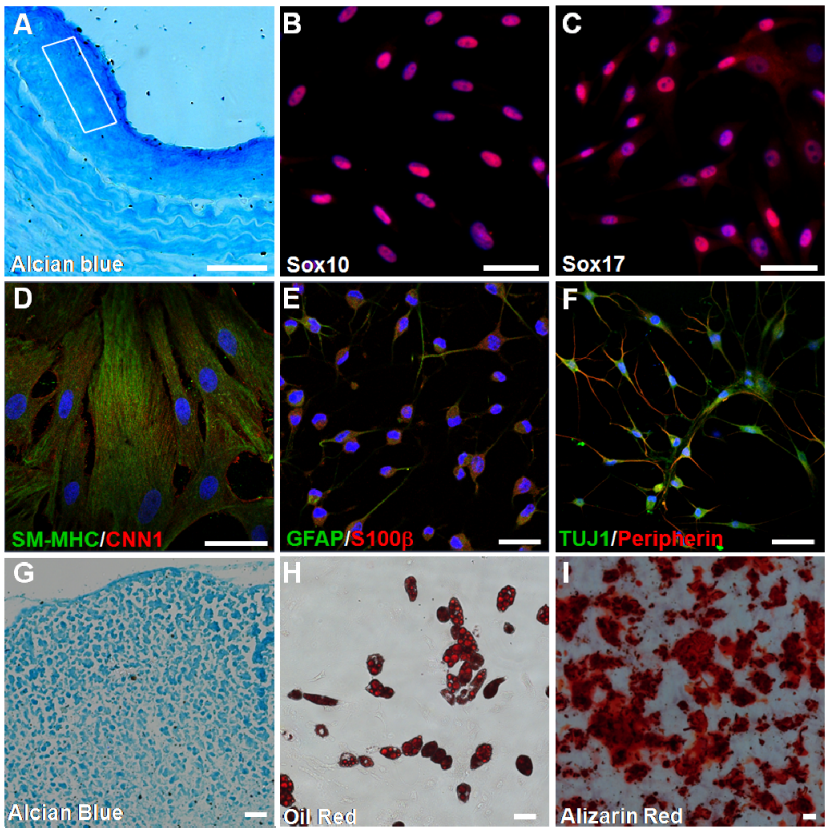

Figure 3.9. Characterization of MVSCs from neointima in rat. (A) Alcian blue staining of a cross-section of carotid artery from SD rat at week 5 after injury. Square indicates the area where the cells were isolated. Scale bar is 50 μm. (B-C) The cells isolated from neointima in rat were stained for MVSC markers Sox10 and Sox17. Scale bars are 50 μm. (D-I) The cells isolated from neointima were subjected to differentiation assays and stained for SMC markers SM-MHC and CNN1 (D), Schwann cell markers GFAP and S100β (E), neuronal marker TUJ1 and peripherin (F), aggrecan in chondrogenic culture by using alcian blue (G), oil droplets in adipogenic culture by using oil red (H), and calcified matrix in osteoblastic culture by using alizarin red) (I). Scale bars of D-F are 50 μm. Scale bars of G-I are 100 μm.

of ectopic cartilage tissue formation in the injured blood vessels.

To determine whether there were still undifferentiated MVSCs in neointima, we isolated cells from neointima tissue at 1 month after injury by using the tissue explant culture method. Indeed, cells with same marker expression and differentiation potential as MVSCs could be derived from neointima tissues (Figure 3.9B-I), suggesting that MVSCs were capable of self-renewal *in vivo* during vascular remodeling.

3.7 Conclusion

In this chapter, we provided compelling evidence to show that previously identified synthetic/proliferative SMCs are derived from differentiation of MVSCs rather than de-differentiation of contractile SMCs. Upon vascular injury, MVSCs are activated to proliferate and differentiate to contribute to vascular remodeling and diseases. The findings provide a new perspective on vascular biology, and may lead to the development of new therapies for vascular diseases. More importantly, our finds suggest a new hypothesis: Vascular disease might be stem cell disease. Since our study is first and only one in this field, further studies using different conditions and animal models are needed to verify this important discovery.

Chapter 4. MVSCs exist in human vessels

4.1 Comments from mass media

After the publication of our study in Nature Communications[23], there were many reports/comments from mass media. In the report from UC Berkeley News Center[66], Dr. Deepak Srivastava, who directs cardiovascular and stem cell research at the Gladstone Institutes in San Francisco said: "This is groundbreaking and provocative work, as it challenges existing dogma. Targeting the vascular stem cells rather than the existing smooth muscle in the vessel wall might be much more effective in treating vascular disease." As well, Dr. Shu Chien, director of the Institute of Engineering in Medicine at UC San Diego said: "If your target is wrong, then your treatment can't be very effective. These new findings give us the right target and should speed up the discovery of novel treatments for vascular diseases."

However, as pointed out by experts in this field, the data in animals may not be directly translated into human. Therefore, it is critical to prove this concept that MVSCs contributes to vascular diseases in human. We collected clinical samples and performed cell isolation, immunostaining and differentiation to identify human MVSCs. In addition, we also performed cryosectioning and immunostaining to verify the existence of MVSCs in diseases.

4.2 Methods and Materials

Cell isolation

Human carotid arteries were obtained from National Disease Research Interchange (Philadelphia, PA). The cells isolation methods were described previously[40]. Briefly, the tissue segments were washed three times with PBS supplemented with 1% P/S. The surrounding connective tissues and adventitia were dissected away under a dissecting microscope. Endothelium was removed by scraping off the cell layer on the luminal surface with sterile scalpel blades. For tissue explant culture method, the tunica media was cut into mm-size and placed onto the surface coated with 1% CellStart in 6-well plates. The cells were cultured in DMEM with 5% FBS, 20 ng/ml bFGF and 20ng/ml EGF. Cells were then seeded onto CellStart-coated dishes and maintained at 37°C in an incubator with 5% CO_2. For the directed differentiation of human MVSCs into peripheral neuron like cells, Schwann cell like cells, osteoblasts, adipocytes and chondrocytes, the cells were incubated in specific induction media described previously for 2-3 weeks [24,41].

Immunostaining and dye staining

For immunostaining, cells were fixed with 4% PFA, permeabilized with 0.5% Triton X-100, and blocked with 1% BSA. Samples were incubated with specific

primary antibodies (Table 2.2) for 2 hours at room temperature, washed with PBS for 3 times, and incubated with appropriate Alexa 488- and/or Alexa 546-labeled secondary antibodies. Nuclei were stained with DAPI. Fluorescence images were collected by a Zeiss LSM710 confocal microscope. For organic dye staining, cells were fixed with 4% PFA for 30 min, washed and stained with alizarin red, alcian blue, oil red or Verhoeff's dye according to the instruction of the manufacturers. Images were collected by a Zeiss Axioskop 2 plus microscope.

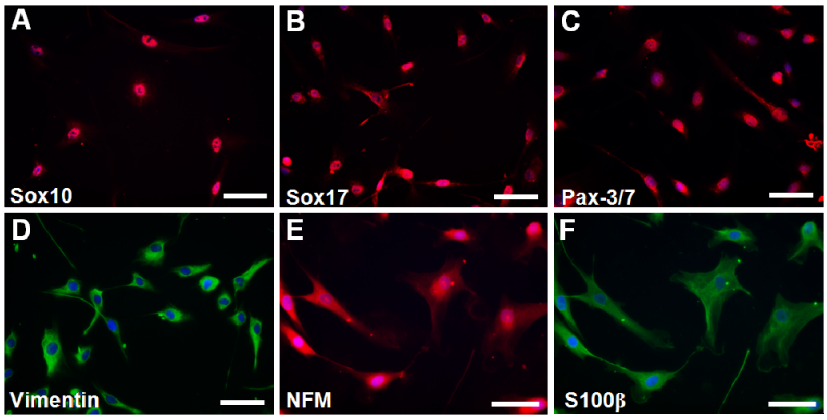

Figure 4.1. Marker expression of human MVSCs isolated from carotid artery. Immunostaining of MVSCs isolated from human carotid arteries with antibodies against Sox10, Sox17, Pax-3/7, vimentin, NFM and S100β. Scale bars are 100 μm.

4.3 Identification and characterization of human MVSCs

To date, we collected over 50 human artery samples. Here we used the data from a healthy carotid artery as representative. Mouse and rat blood vessels are too small to accurately isolated adventitia layer, tunica media and endothelial layers. In contrast, human tissues are large enough for us to separate these layers to determine the location of MVSCs. By using tissue explants culture method, we successfully isolated human MVSCs from both the adventitia layer and tunica media of carotid artery, aorta and coronary artery, indicating that MVSCs locate in both the adventitia and medium layers. Lineage tracing experiment using Sox10 as marker also confirmed the location of MVSCs in both adventitia and medium layers[67].

Immunostaining showed that cells isolated from human arteries expressed MVSC markers such as Sox10, Sox17, Pax-3/7, vimentin, NFM and S100β (Figure 4.1). Similar to rodent MVSCs, human MVSCs can be induced to differentiate into Schwann cell like cells, neuron like cells, SMCs, chondrocytes and adipocytes (Figure 4.2). However, it is worth noting that MVSCs isolated from patients with different ages differs in multipotency (data not shown). Further studies are required to investigate the differences between these samples.

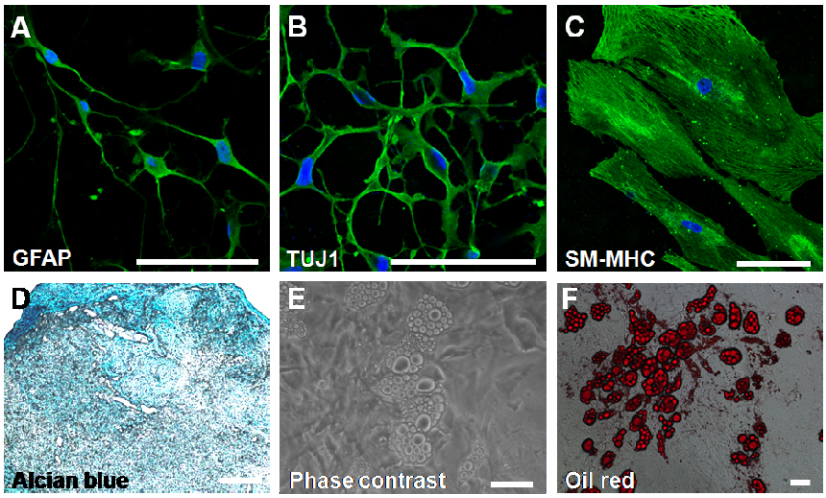

Figure 4.2. Differentiation assay of MVSCs derived from human carotid artery. (A) Human MVSCs derived Schwann cell like cells were stained with an antibody against GFAP (B), peripheral neuron like cells were stained with an antibody against TUJ1 (C), SMCs were stained with an antibody against SM-MHC (D), chondrocytes were stained for aggrecan by using alcian blue (E), phase contrast picture of oil drops (F), adipocytes were stained for oil droplets by using oil red staining (G). Scale bars are 100 μm.

4.4 Comparison of human MVSCs and human SMC line

Previous theory suggests that the phenotypic modulated SMCs, which barely grow in the first week of the primary culture, account for a sudden cell expansion afterwards, and that these expanded cells can undergo re-differentiation under the same culture condition. These expanded cells are traditionally characterized as “proliferative/synthetic SMCs”, assuming that they are derived from mature SMCs. Our findings imply that SMCs in many previous *in vitro* studies may be derived from MVSCs. To further prove this, a commercially available human aortic SMC line were subjected to Immunostaining and showed that the cells expressed low level of Sox10—a MVSC marker, suggesting that these cells are very likely derived from MVSCs. In contrast, human MVSCs of primary culture have higher level of Sox10 expression and low level of SMA that is not incorporated into stress fibers[67]. There are over 40,000 papers on vascular SMCs. If the “proliferative/synthetic SMC” was derived from MVSCs, many previous conclusions on SMCs may need to be revisited.

4.5 Conclusion

In summary, we identified MVSCs in human arteries, which showed similar characteristics of rat/mouse MVSCs in the aspects of marker expression and multipotency. Furthermore, we found that human MVSCs also participated into neointimal hyperplasia, ectopic cartilage formation as well as the plaque formation in atherosclerosis (Data not shown). These finds

confirmed the importance of MVSCs in the pathogenesis of vascular diseases. Moreover, the isolation of human MVSCs facilitates the discovery of new drugs and therapies with the proliferation, migration and aberrant differentiation of MVSC as targets. Again, since we are the first and only one to show evidence supporting this new theory, more clinical samples with different vascular diseases are required to validate this.

Chapter 5. Sox10^{+} stem cells contribute to wound healing

5.1 Motivation

Despite their importance in wound healing and scar formation, fibroblasts and myofibroblasts are mainly characterized by cell morphology, ultra-structures including extensive cell-matrix adhesion, abundant intercellular adherens and bundles of contractile cytoplasmic microfilaments such as non-muscle myosin[68]. To date, there is no detailed characterization such as transcriptome, specific surface markers as well as the suitable culture condition to maintain specific phenotype. Moreover, the sources of myofibroblasts existing in order to meet the temporarily high demand for contractile cells in wound repair remains controversial. Besides local fibroblasts in dermis[69], pericytes and vascular SMCs[70], epithelial cells through EMT, and bone marrow cells, it is reasonable to investigate whether tissue specific stem cells could be another possible origin of myofibroblasts. Therefore, in this chapter, we investigated the cell types participated in the general dermal wound healing as well as the remodeling of tissue engineered scaffolds and identified a novel type of stem cells showing similar characteristics with NCSCs. This type of stem cells could spontaneously differentiate into myofibroblasts *in vitro* and *in vivo* to form the capsule layer around skin wound and transplanted biomaterials.

5.2 Methods and materials

In vivo transplantation

To produce single-polymer PLLA (1.09 dL/g inherent viscosity) (Lactel Absorbable Polymers, Pelham, AL) nanofibrous scaffolds, we used electrospinning as described previously[71]. The derived nanofibrous scaffolds were transplanted subcutaneously at different locations. The rats were sacrificed at different time points after transplantation. For the transplantation of microfibrous vascular grafts[60], the vascular grafts were transplanted into athymic rats by using left common carotid artery anastomosis.

Cell isolation

The segments of explanted grafts and scaffolds were washed three times with PBS supplemented with 1% P/S. Then the tissues segments ware cut into mm-size and placed onto the surface coated with 1% CellStart in 6-well plates and maintained at 37°C in an incubator with 5% CO_2. The cells were cultured in DMEM with 2% CEE, 1% FBS, 1% N2, 2% B27, 100 nM RA, 50 nM 2ME, 1% P/S and 20 ng/ml bFGF. Cells migrated out from the tissues within 3 days.

Immunostaining and dye staining

For immunostaining, cells or tissue sections were fixed with 4% PFA, permeabilized with 0.5% Triton X-100, and blocked with 1% BSA. Samples

were incubated with specific primary antibodies (Table 2.2) for 2 hours at room temperature, washed with PBS for 3 times, and incubated with appropriate Alexa 488- and/or Alexa 546-labeled secondary antibodies. Nuclei were stained with DAPI. Fluorescence images were collected using a Zeiss LSM710 confocal microscope. For organic dye staining, cells were fixed with 4% PFA for 30 min, washed and stained with alizarin red, alcian blue, or oil red according to the instruction of the manufacturers. Images were collected using a Zeiss Axioskop 2 plus microscope.

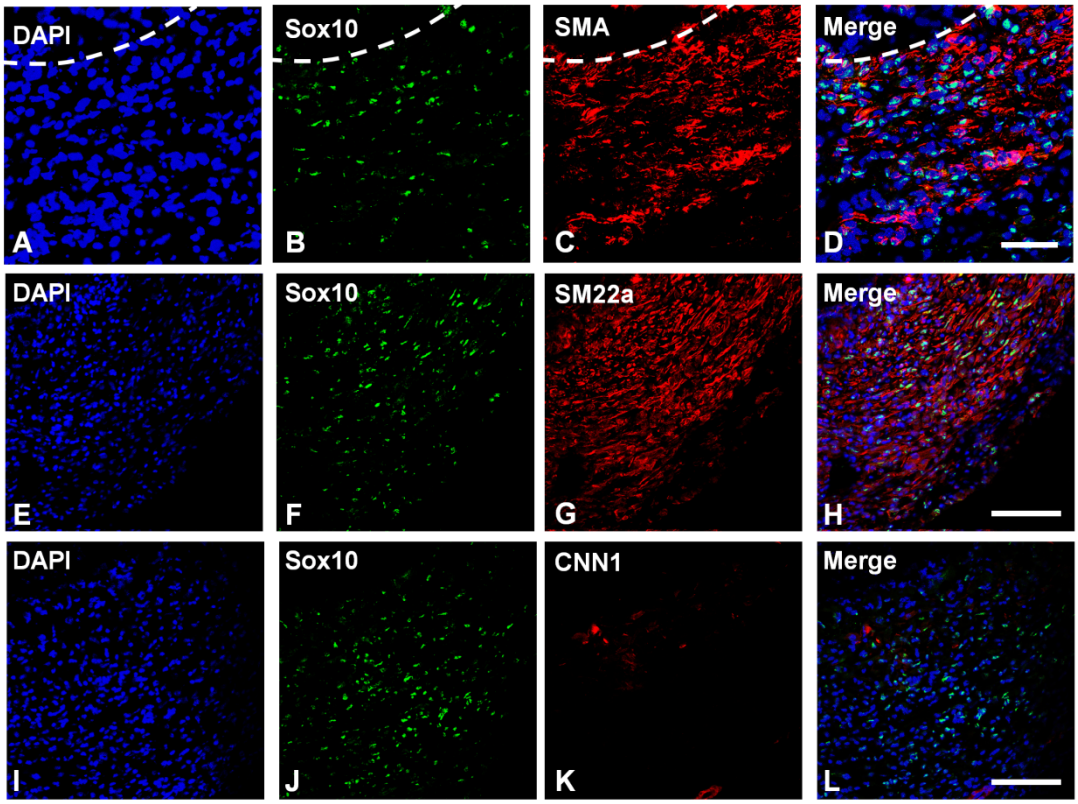

Figure 5.1. Identification of Sox10$^+$ stem cells participated in the remodeling of vascular graft. At 10 days after implantation, stem cell population was identified by immunostaining for stem cell marker Sox10 (B, F, J) with early SMC marker SMA (C), SM22α (G), and medium stage SMC marker CNN1 (K). Dashed lines indicate the border between the graft (top part) and the outer layer. Scale bars in A-D are 100 μm. Scale bars in E-L are 50 μm.

5.3 Sox10$^+$ cells participated into the remodeling of vascular grafts

After we discovered MVSCs in blood vessel, we hypothesized that MVSCs will participate into the remodeling of artificial vascular grafts to form mature SMC layers outside the grafts. Therefore, we explanted the nanofibrous vascular grafts at 10 days after transplantation and performed cryosectioning. Immunostaining showed that majority of cell outside the grafts expressed Sox10 (Figure 5.1) as well as general SMC marker including SMA (Figure 5.1C) and SM22α (Figure 5.1G), but not intermediate marker such as CNN1 (Figure 5.1K), indicating the cells are at early differentiation stage. At 1

month after transplantation, majority of the cells differentiated into mature SMCs, as evidenced by the expression of CNN1 and SM-MHC, suggesting that these Sox10$^+$ cells may differentiate into mature SMCs to participate into the vascular maturation[72].

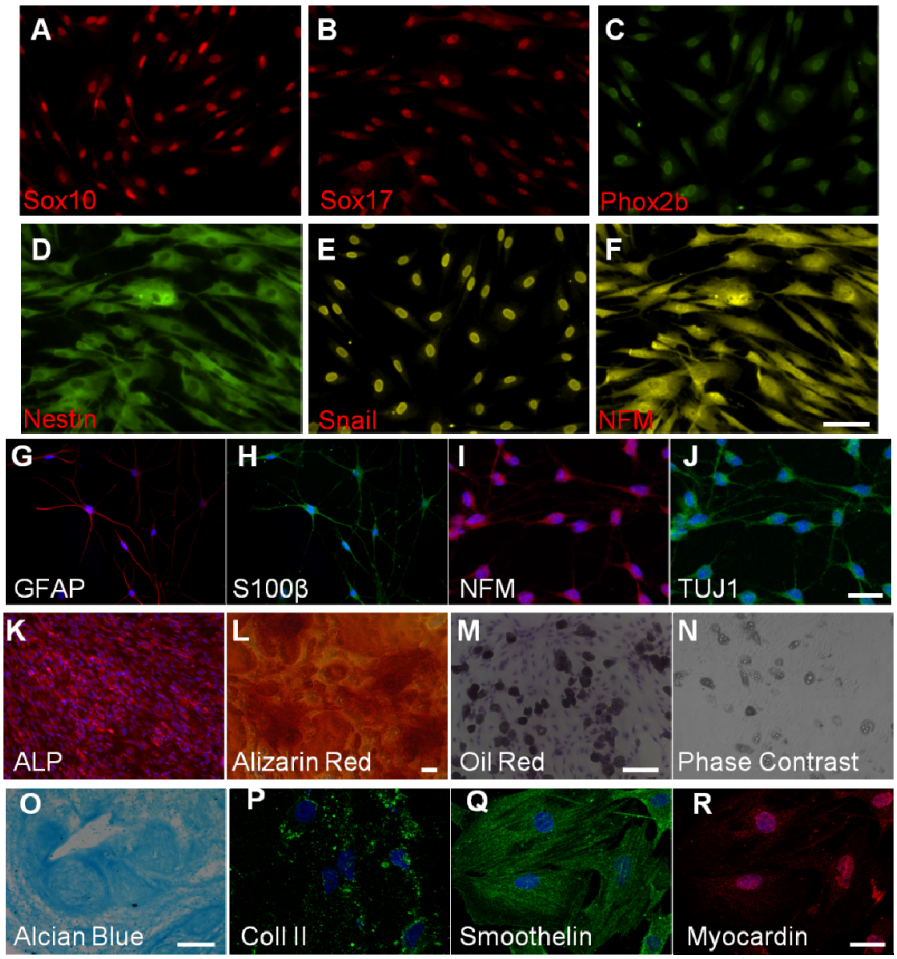

Figure 5.2. Marker expression and multipotency of isolated Sox10$^+$ cells. (A-F) The isolated cells were immunostained with antibodies against Sox10, Sox17, Phox2b, Nestin, Snail and NFM. Scale bar is 100 μm. (G-R) The isolated cells isolated were subjected to differentiation assays and stained for Schwann cell markers GFAP and S100β, neuronal marker NFM and TUJ1, calcified matrix in osteoblastic culture by using alizarin red and ALP, oil droplets in adipogenic culture by using oil red, aggrecan in chondrogenic culture by using alcian blue and collagen II, and SMC markers smoothelin and myocardin. Scale bars for G-J, and Q-R are 50 μm. Scale bars for K-P are 100 μm.

5.4 Characterization of the Sox10$^+$ cells

To determine whether these Sox10$^+$ cells are identical to previously identified MVSCs, we performed cell isolation by using tissue explants culture method. The isolated cells were subjected to antibody screening. Immunostaining showed that cells expressed MVSC markers such as Sox10, Sox17, Phox2b, nestin, snail and NFM (Figure 5.2A-F). Similar to MVSCs, the isolated Sox10$^+$ cells can be induced to differentiate into Schwann cell like cells (GFAP$^+$/S100β$^+$), neuron like cells (NFM$^+$/TUJ1$^+$), osteoblasts

(ALP$^+$/Alizarin red$^+$), adipocytes (Oil red$^+$) and chondrocytes (Aggrecan$^+$/collagen II$^+$) (Figure 5.2G-P), indicating that they are identical to MVSCs. Moreover, we also tested whether the default differentiation pathway of the isolated Sox10$^+$ cells are myofibroblasts in regular culture medium. As expected, they spontaneously differentiated into SMA$^+$/CNN1$^+$ cells (Data not shown) and subsequently into myocardin$^+$/smoothelin$^+$ SMCs in culture (Figure 5.2Q-R), indicating that they might be the precursor of SMCs/myofibroblasts.

Although the isolated Sox10$^+$ cells showed similar characteristics with MVSCs, it is unknown that whether this type of stem cells represents a unique stem cell type outside blood vessels. Therefore, we performed cell isolation from other tissues with tissue explants culture method and found that many tissues including skeletal muscle, liver, and the connective tissues (Data not shown), indicating that Sox10$^+$ cell population exists all over the body. Then we raised the question: where are the Sox10$^+$ cells observed in vascular grafts from?

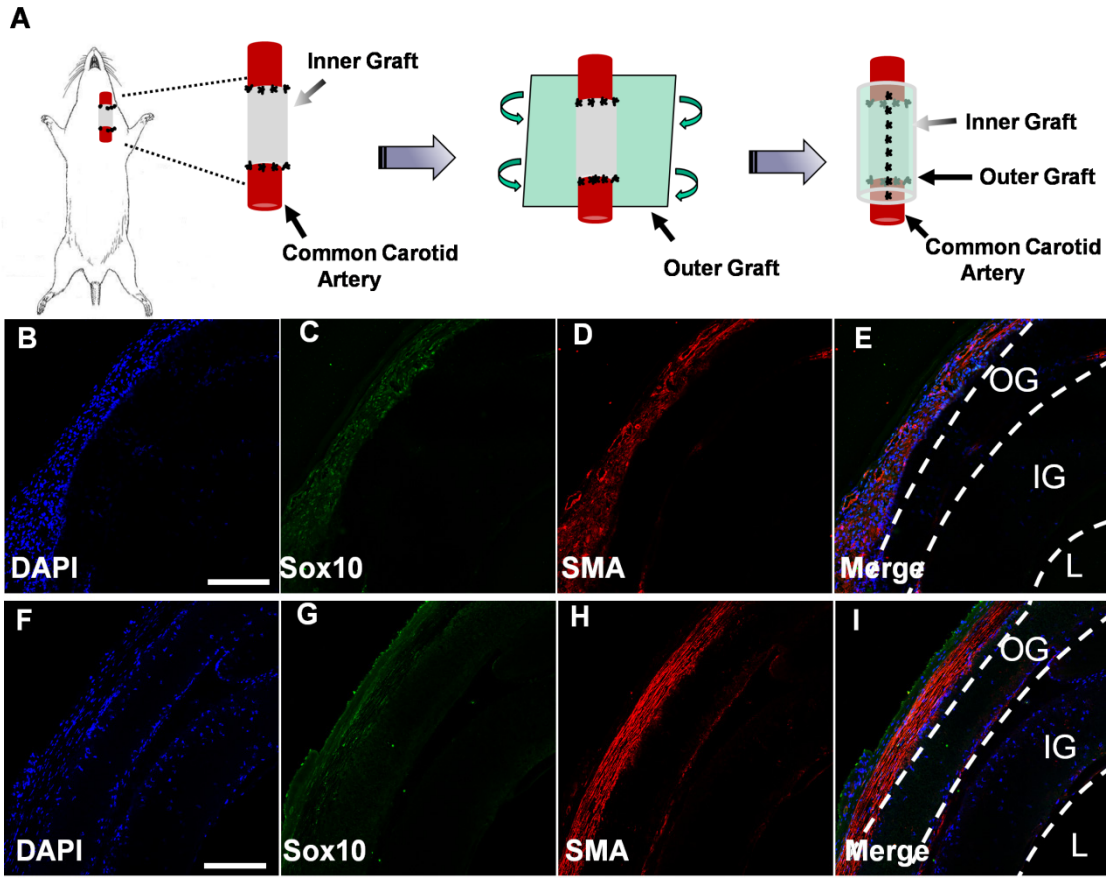

Figure 5.3. Origins of the Sox10$^+$ cells in vascular grafts. A. Schematic illustration of the engineered bi-layer vascular grafts. B-I. Immunostaining of sections of the bi-layer grafts at 10 days (B-E) and 1 month (F-I) after transplantation with antibodies against Sox10 and SMA. Scale bars are 50 μm.

5.5 Origins of the Sox10$^+$ cells

There are two possible sources of the Sox10$^+$ cells we identified in the

vascular grafts. One is from two ends of the native blood vessels, and the other one is from the surrounding tissues. Therefore, we engineered a bi-layer vascular graft, in which the outer layer is longer than the inner graft to block the cell migration from surrounding tissues (Figure 5.3A). At 10 days after transplantation, immunostaining showed that there indeed exist Sox10$^+$ cells on the surface of the outer layer but not the inner graft (Figure 5.3B-E), indicating that at early time point, surrounding tissues are the major source of the Sox10$^+$ cells participated in the remodeling of vascular grafts. In contrast, at 1 month after transplantation, immunostaining showed that Sox10$^+$ cells can be observed in both the outer layer and the space in between the two grafts (Figure 5.3F-I), indicating that the cells derived from blood vessels are not the major source.

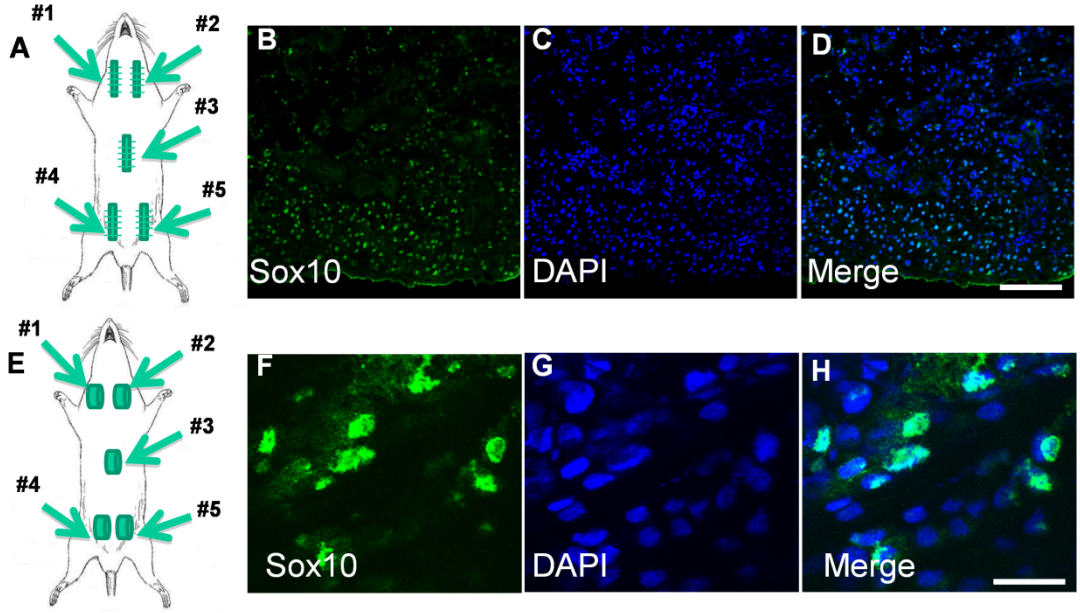

Figure 5.4. Involvement of Sox10$^+$ cells in wound healing and tissue engineering. (A-D) Creation of skin wounds in rat. The sections were immunostained with antibodies against Sox10. Scale bar is 100 μm (E-H) Transplantation of nanofibrous scaffolds subcutaneously into rats. The sections were immunostained with antibodies against Sox10. Nuclei were stained with DAPI. Scale bar is 50 μm.

5.6 Sox10$^+$ cells participated into general wound healing

Since there exist Sox10$^+$ stem cells in surrounding tissues besides blood vessels, and this type of stem cells is likely the precursor of myofibroblasts. We then further test the hypothesis that this type of stem cells exists all over the body and participate into general wound healing process. Therefore, we utilized a skin wound model and did immunostaining extensively to examine whether there are Sox10$^+$ cells involved. As shown in Figure 5.4A-D, we created skin wound all over the body of SD rat and found large amount of Sox10$^+$ cells in the area of skin wound, indicating that Sox10$^+$ cells are a major population involved in wound healing process. Moreover, we also implanted nanofibrous scaffolds to determine whether the Sox10$^+$ cells can also

participated into the remodeling of biomaterials. Immunostaining also confirmed the recruitment of $Sox10^+$ cells into biomaterials, which is independent of the location (Figure. 5.4E-H). Lineage tracing experiments using Sox10 as marker further showed that the $Sox10^+$ cells participated into the scar formation in wound healing process (Data not shown).

In addition, to confirm the $Sox10^+$ cells are the similar stem cell type as we identified before, we performed cell isolation and characterized these cells. Immunostaining showed that they indeed express Sox10, Sox17, Phoxb2, snail, nestin and NFM (Data not shown).

5.7 Conclusion

In summary, we identified a type of $Sox10^+$ adult stem cells similar to MVSCs, which express stem cell markers, have multipotency, and can spontaneously differentiate into myofibroblasts and SMCs. Extensive immunostaining confirmed the participation of this type of stem cells into wound healing and the remodeling of biomaterials. Our findings suggest that this type of stem cells might be the precursors of the previously identified myofibroblasts, which proved the concept that local tissue specific stem cells are at least one of sources of myofibroblasts. However, further lineage tracing studies are required to elucidate the function of this type of stem cells in wound healing such as tissue fibrosis. In addition, the relative contribution of this type of stem cells and other reported precursors to wound healing also needs further investigation.

Chapter 6. Synovial stem cells and their response to porosity of microfibrous scaffold

6.1 Motivation

Tissue specific stem cells hold great promising for *in situ* tissue regeneration and it is critical to understand the cell-biomaterial interaction. Efficient stem cell differentiation is necessary to produce functional tissues. However, one major obstacle for engineering 3D functional tissue is the poor understanding of the effects of scaffolds on stem cell differentiation and commitment to specific cell lineages. Many soluble biochemical stimuli, such as RA, growth factors, and cytokines, can be used to direct stem cell differentiation [50]. However, during the *in vivo* tissue regeneration process, not only biochemical soluble signals, but also macromolecular components of extracellular matrix as well as physical cues may play important role in defining and guiding the stem cell differentiation. Despite its importance, the effects of scaffolds on stem cell behaviors including proliferation, infiltration and differentiation are not well understood.

In this study, we identified precursor of MSCs from rat knee joint synovial membrane, named neural crest cell like synovial stem cells (NCCL-SSCs). NCCL-SSCs show characteristics of NCSCs, express markers including Sox10, Sox17 and S100β, are cloneable, and can differentiate into neural lineages as well as mesenchymal lineages. In addition, electrospun composite scaffolds with improved porosity were produced by using PLLA as structural and PGA as sacrificial material. Lineage specific genes were differentially regulated by scaffolds with different porosity without specific chemical cues, indicating lineage specification by properties of scaffolds.

6.2 Method and materials

Cell isolation

The synovial membrane was isolated from SD rat knee joint under dissecting microscope. Tissue segments were washed three times with PBS supplemented with 1% P/S. Then the tissues segments ware cut into mm-size and placed onto the surface coated with 1% CellStart in 6-well plates and maintained at 37°C in an incubator with 5% CO_2. The cells were cultured in DMEM with 2% CEE, 1% FBS, 1% N2, 2% B27, 100 nM RA, 50 nM 2ME, 1% P/S and 20 ng/ml bFGF. Cells migrated out from the tissues within 3 days.

Immunostaining and dye staining

For immunostaining, cells were fixed with 4% PFA, permeabilized with 0.5% Triton X-100, and blocked with 1% BSA. Samples were incubated with specific primary antibodies (Table 2.2) for 2 hours at room temperature, washed with PBS for 3 times, and incubated with appropriate Alexa 488- and/or Alexa 546-labeled secondary antibodies. Nuclei were stained with DAPI.

Fluorescence images were collected using a Zeiss LSM710 confocal microscope. For organic dye staining, cells were fixed with 4% PFA for 30 min, washed and stained with alizarin red, alcian blue, or oil red according to the instruction of the manufacturers. Images were collected using a Zeiss Axioskop 2 plus microscope.

Flow cytometric analysis

For flow cytometric analysis, cells were dissociated after the exposure to 0.2% EDTA for 20 min at room temperature. The cells in suspension were blocked with 1% BSA, incubated with specific pre-conjugated primary antibodies against CD29 (BD pharmingen) and CD44 (BD Pharmingen). Negative control sample was incubated with a non-specific antibody with the same isotype as the specific primary antibody, and stained with the same secondary antibody. 7-AAD was used to exclude dead cells. Cells were analyzed by using FACScan flow cytometer and FlowJo software.

Single cell cloning and stem cell differentiation

For the clonal assays, cells were detached, and resuspended with maintenance medium and filtered through membranes with 40-μm pore size to obtain single cells. Filtered cells were seeded onto CellStart-coated 96-well plates at the clonal density (1 cell/well) and cultured for 3 weeks at 37°C in an incubator with 5% CO_2. For the directed differentiation into peripheral neurons, Schwann cells, osteoblasts, adipocytes and chondrocytes, the cells were incubated in specific induction media described previously for 1-3 weeks [24,41].

Generation of transgenic mice and genotyping

All experimental procedures with animals were approved by the ACUC committee at University of California, Berkeley. NIH guidelines for the care and use of laboratory animals have been observed. Transgenic mice, expressing Cre recombinase under the control of the Wnt1 promoter were mated with Rosa26-loxP-yellow fluorescence protein (YFP) mice to generate Wnt1-Cre/loxP-YFP mice. Genotyping was performed with PCR by using total DNA extracted from mice tail tissues as described previously [73].

RNA Isolation and qPCR

To directly explore the effect pore size of scaffold on lineage specific gene expression of stem cells, approximately 1,000,000 cells were seeded on 3-cm x 3-cm scaffolds and cultured in spontaneous differentiation media (DMEM with 10% FBS and 1% P/S) for 1 week. Cells were then lysed with Trizol reagent and total RNA was extracted as previously described[42]. For qPCR, RNA pellets were resuspended in DEPC-treated H_2O. cDNA was synthesized by using two-step reverse transcription with the ThermoScript RT-PCR system (Invitrogen), followed by qPCR with SYBR green reagent and the ABI Prism

7000 Sequence Detection System (Applied Biosystems). The sequences of the primers used in this study are shown in Table 6.1.

Table 6.1. Primer sequences used in this study.

Gene	Forward	Reverse
Collagen II	CCAGGGCTCCAATGATGTG	GTGTTTCGTGCAGCCATCCT
Aggrecan	CTTCAAGCTGAACTATGACCACTTTACT	CATGGTCTGGAACTTCTTCTGAGA
BGLAP	GCAGACCTAGCAGACACCATGA	AGGTCAGAGAGGCAGAATGCA
Runx2	TCAATGGTTGGGAGAGAAGCA	CCTTCTGCACCTCCTTTAGCA
SMA	TCCTGACCCTGAAGTATCCGATA	GGTGCCAGATCTTTTCCATGTC
CNN1	AGAACAAGCTGGCCCAGAAA	CACCCCTTCGATCCACTCTCT
PPARγ	CGAGCCCTGGCAAAGCATTTGTAT	TGTCTTTCCTGTCAAGATCGCCCT
LPL	ACAGTCTTGGAGCCCATGCT	CAAGCCAGTAATTCTATTGACCTTCTT
18S	GCCGCTAGAGGTGAAATTCTTG	CATTCTTGGCAAATGCTTTCG

Statistical Analysis

The data are presented as mean ± s.d.. All data were compared by using one-way ANOVA tests. Holm's t test was then performed to evaluate significant differences among the scaffold groups. *P* value less than 0.05 was considered statistically significant.

6.3 Cell isolation and characterization

We dissected the synovial membrane from rat knee joint under dissecting microscope and used tissue explant culture method to isolate stem cells with a modified medium for MVSCs. The isolated synovial cells showed a fibroblast-like, spindle shaped morphology, which is similar to previously reported synovial MSCs (Figure 6.1A-B). The isolated cells express general MSC markers including CD29 and CD44 as evidenced by flow cytometric analysis (Figure 6.1C-D). To further characterize the marker expression of the isolated synovial cells, we performed protein marker expression screening with over 50 antibodies and found that the isolated cells also express neural crest markers including Sox10, snail, Pax-3/7, Slug, Vimentin, endoderm markers Sox17, glial cell marker S100β, and neural cell marker NFM (Figure 6.1E-M), suggesting that the isolated cells might not be exactly the same with previously reported MSCs.

To determine whether the isolated cells possess multipotency as NCSCs, the cells were cultured with specific induction media for 1-4 weeks. Immunostaining showed that the isolated cells can differentiate into $GFAP^+/S100\beta^+$ Schwann cell like cells (Figure 6.2A, B), $NFM^+/TUJ1^+$ peripheral neuron like cells (Figure 6.2C, D) when cultured with specific induction media for 1 week, indicating that the isolated cells have the capability of differentiation into ectodermal lineages. In addition, to test the potential of differentiation into SMCs, we co-cultured the isolated cells with OP9-Delta-1 cell line for 2 weeks[23]. Immunostaining showed that the differentiated cells formed dense stress fibers and expressed SMA and SM-MHC (Figure 6.2E, F), indicating differentiation into mature SMCs. To test the potential into chondrocytes, we cultured the cells as pellets with 10 ng/ml TGF-β3 for 3

weeks. Alcian blue staining with sections of cell pellets showed significant aggrecan synthesis (Figure 6.2G). Immunostaining also showed significant collagen II expression in the cell pellets (Figure 6.2H), indicating differentiation into mature chondrocytes. After we cultured the cells with insulin for 3 weeks, obvious oil droplets were found in culture (Figure 6.2I). Oil red staining also confirmed the differentiation into adipocytes (Figure 6.2J).

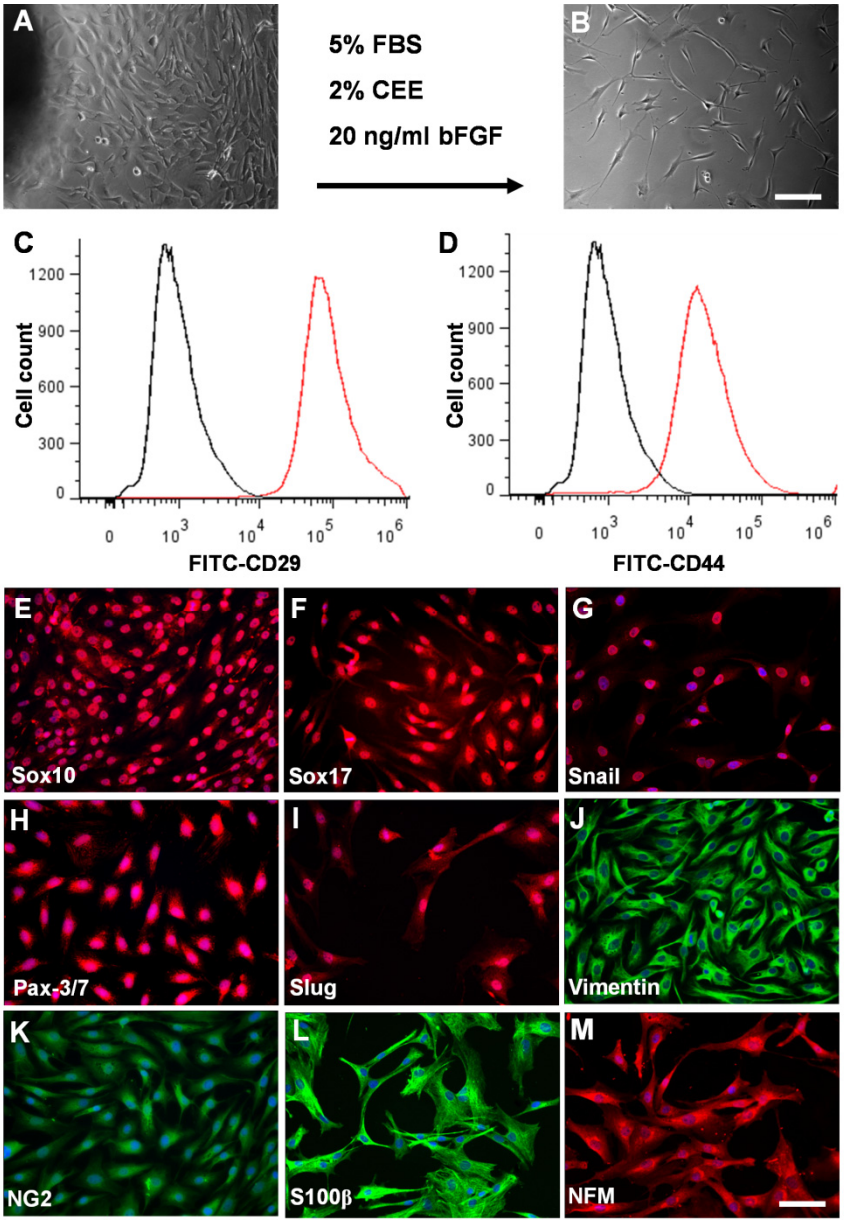

Figure 6.1. Isolation and characterization of NCCL-SSCs. (A-B) Phase contrast images of NCCL-SSCs isolated by using tissue explants culture methods before and after passaging. Scale bar is 200 μm. (C-D) Flow cytometric analysis of isolated synovial cells by using antibodies against CD29 and CD44. (E-M) Immunostaining of isolated cells by using antibodies against Sox10, Sox17, Snail, Pax-3/7, Slug, Vimentin, NG2, S100β and NFM. Scale bar is100 μm.

After cultured with osteogenic medium for 3 weeks, the cells showed

significant calcification (Figure 6.2K). Alizarin red staining also confirmed the differentiation into mature osteoblasts (Figure 6.2L). Therefore, the isolated cells cannot only differentiate into mesenchymal lineages including SMCs, chondrocytes, adipocytes and osteoblasts as previously reported, but also differentiate into neural lineages, similar to NCSCs. Therefore, we named this type of cell as neural crest cell like synovial stem cells (NCCL-SSCs).

6.4 Single cell cloning assay of NCCL-SSCs

To investigate whether the derived NCCL-SSCs is a single stem cell type with multipotency or a mixture of different progenitor cells, we performed single cell cloning with maintenance culture medium. The NCCL-SSCs were detached and seeded into 96 well plates at cloning density (1 cell/well) and cultured for 3 weeks. The average plating efficiency is about 10%, and the derived colonies uniformly express aforementioned markers including but not limited to Sox10 and Sox17 (Figure 6.3A,B). Differentiation assay showed that the cloned NCCL-SSCs can differentiate into Schwann cell like cells, peripheral neuron like cells, SMCs, chondrocytes, adipocytes and osteoblasts (Figure 6.3C-H), indicating that NCCL-SSCs represent one single type of stem cells which expresses markers and has multiple lineage potentials.

Knee joint tissues are generally considered not from neural crest, however, given the fact that NCCL-SSCs possess NCSC properties, we employed lineage tracing model using Wnt1 as a marker to investigate the developmental origin of NCCL-SSCs. After cell isolation from synovial membrane of Wnt-1-Cre/loxP-YFP mouse, we found that the isolated NCCL-SSCs failed to express YFP (Figure 6.3I, J), indicating that NCCL-SSCs are not derived from neural crest.

6.5 Transition to MSC like cells of NCCL-SSCs

To determine the relationship between NCCL-SSCs and previously identified synovial MSCs, we culture the NCCL-SSCs in traditional medium (DMEM+10%FBS) that were widely used to culture synovial MSCs in many previous studies [32,74,75]. TGF-β1, which is a major factor for stem cell differentiation during wound healing process, was also added into the medium to promote the differentiation. After the treatment for 1 week, immunostaining showed that the NCCL-SSCs still retained the expression of some markers including Sox10 and S100β (Figure 7.4A, B), gained the expression of CNN1 (Figure 6.4C), but lost the expression of Sox17 (Figure 6.4D). Flow cytometric analysis showed that the derived cells still retain the expression of the general MSC markers including CD29 and CD44 (Figure 6.4E, F). However, differentiation assay showed that the cells at this stage lost the response to neural and Schwann cell induction media, indicating that they lost the

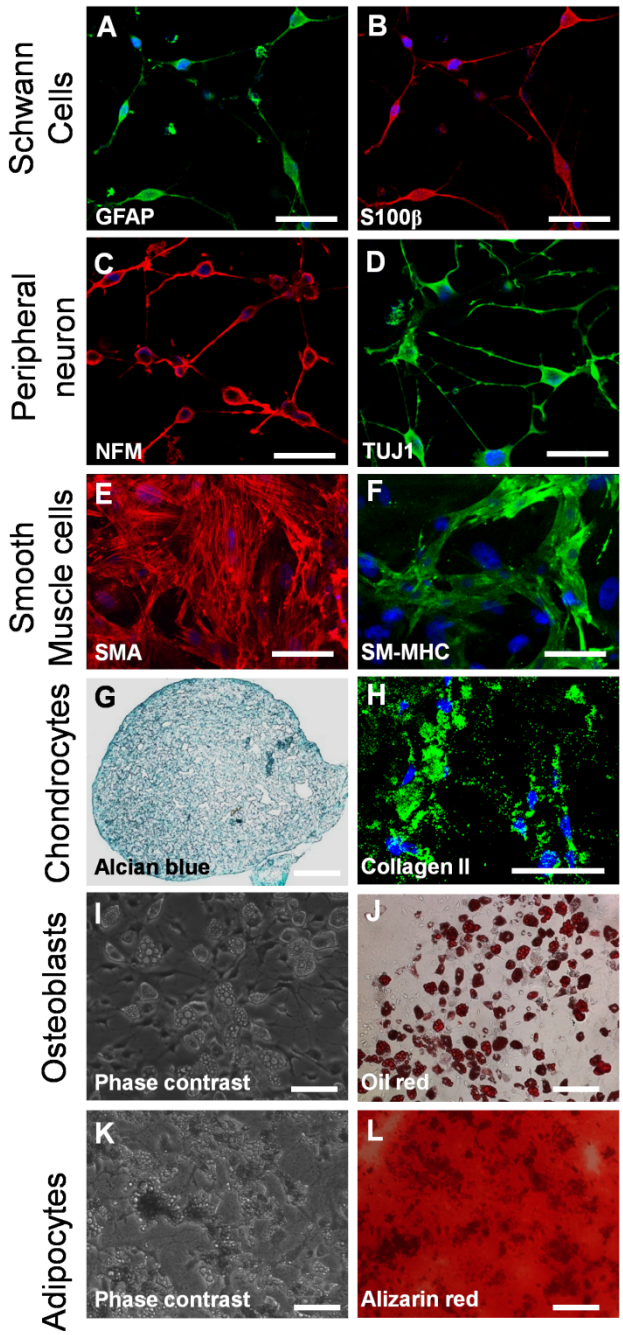

Figure 6.2. Differentiation assay of isolated NCCL-SSCs. (A-B) The isolated synovial cells were cultured in Schwann cell induction medium for 48 hours and were immunostained by using antibodies against GFAP and S100β. Scale bars are 50 μm. (C-D) The isolated synovial cells were cultured in peripheral neuron induction medium for 48 hours and were immunostaining by using antibodies against NFM and TUJ1. Scale bars are 50 μm. (E-F) The isolated synovial cells were co-cultured with OP9-delta1 cells for 2 weeks and were immunostained by using antibodies against SMA and SM-MHC. Scale bars are 100 μm. (G-H) The isolated syonival cells were cultured in chondrogenic induction medium as cell pellet for 3 weeks. The sections of the cell pellet were subjected to alcian blue staining and immunostaining by using an antibody against collagen II. Scale bars are 100 μm. (I-J) The isolated synovial cells were cultured in adipogenic medium for 3 weeks. Phase contrast image and oil red staining were used to show oil droplets. Scale

bars are 100 μm. (K-L) The isolated synovial cells were cultured in osteogenic medium for 3 weeks. Phase contrast image and alizarin red staining were used to show calcium calcification. Scale bars are 100μm.

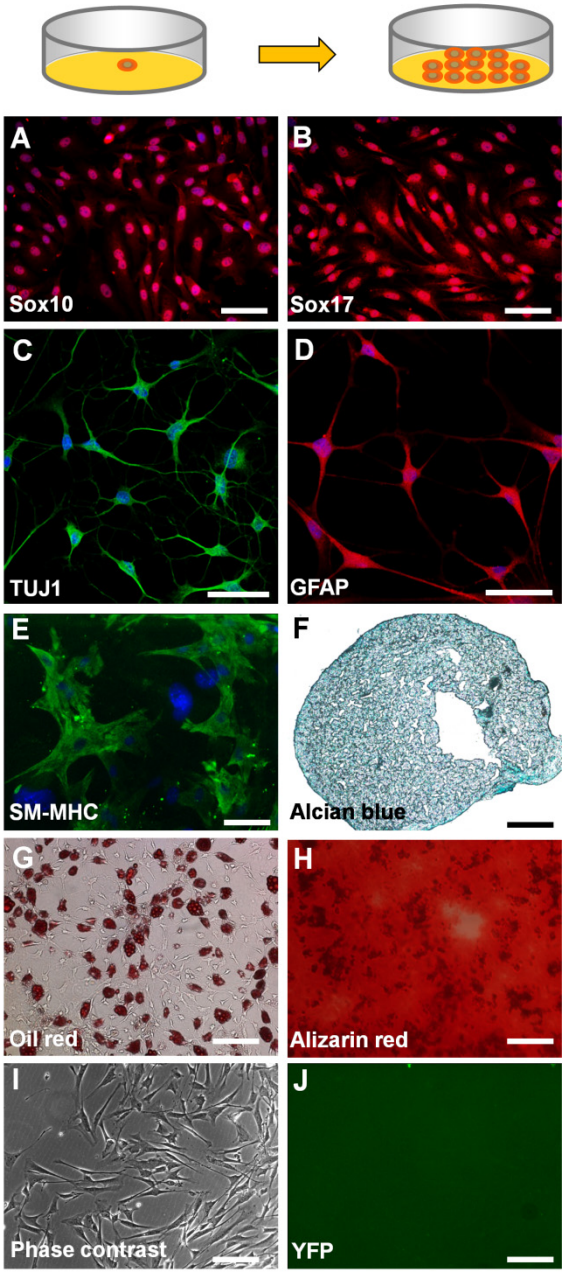

Figure 6.3. Single cell cloning assay of isolated NCCL-SSCs. The isolated synovial cells were plated onto 96 well plates at cloning density and cultured in maintenance medium for 3 weeks. (A-B) The cloned cells were immunostained with antibodies against Sox10 and Sox17. Scale bars are 100 μm. (C-H) The cloned cells were differentiated and characterized as aforementioned. Scale bar is 100 μm in C-E; scale bars are 200 μm in F-H. (I-J) The synovial cells were isolated from Wnt1-Cre/loxP-YFP mice. Phase contrast and fluorescence images were used to show that the isolated synovial cells were not from neural crest. Scale bars are 200 μm.

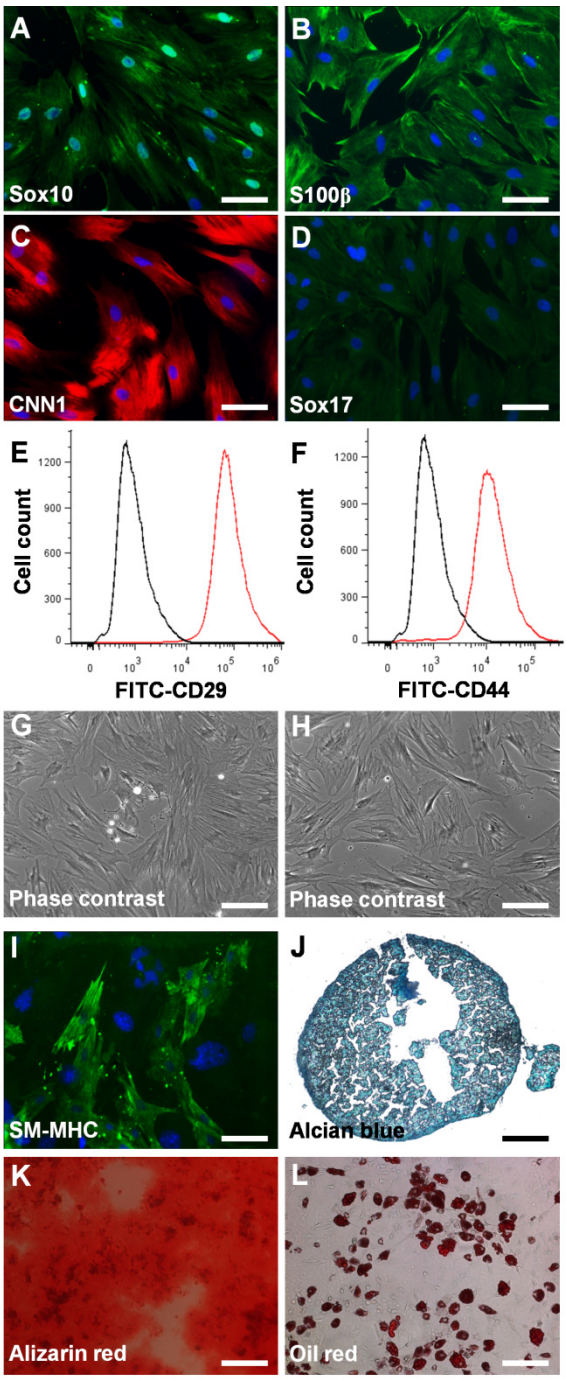

Figure 6.4. Transition to MSC like cells of NCCL-SSCs. The isolated NCCL-SSCs were partially differentiated in DMEM with 10% FBS and 10 ng/ml TGF-β1 for 1 week. (A-D) The differentiated NCCL-SSCs were immunostained with antibodies against Sox10, S100β, CNN1 and Sox17. Scale bars are 100 μm. (E-F) Flow cytometric analysis of partially differentiated NCCL-SSCs with antibodies against CD29 and CD44. (G-H) Phase contrast images were used to show the differentiated NCCL-SSCs cultured with neural and Schwann cell induction media for 2 days. Scale bars are 200 μm. (I-L) The multipotency into mesenchymal lineages of partially differentiated NCCL-SSCs was characterized as aforementioned. Scale bar is 100 μm in I; scale bars are 200 μm in J-L.

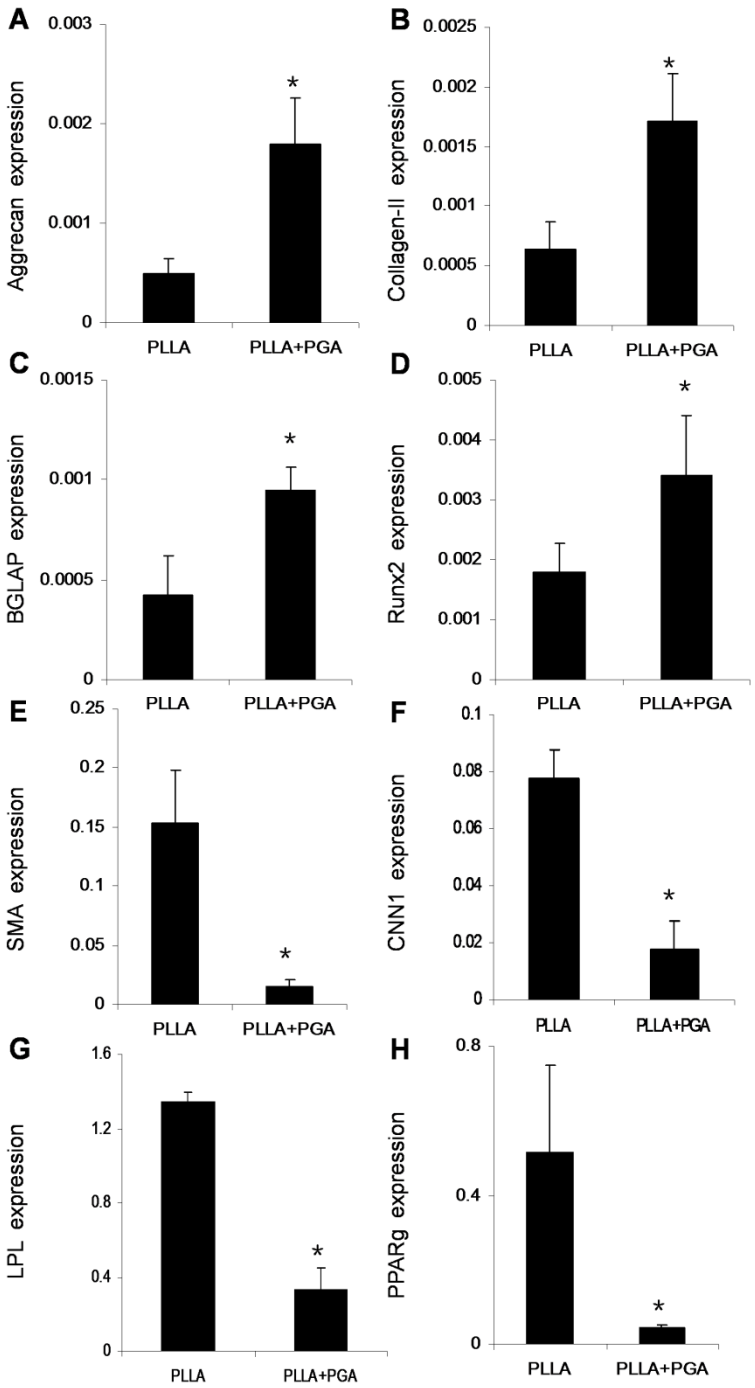

Figure 6.5. Effect of porosity of scaffolds on lineage commitment of NCCL-SSCs. Scaffolds from 4-week PLLA (low porosity) and PLLA/PGA degraded for 4 weeks (high porosity) were selected and used. NCCL-SSCs were seeded and cultured for one week. The cells were lysed and the extracted RNA was subjected to qPCR analysis for gene expression. Expressions of specific lineage markers for chondrocytes (A-B), osteoblasts (C-D), SMCs (E-F) and adipocytes (G-H) were quantified (n=3). * indicates significant difference between PLLA and PLLA/PGA (high) groups (P<0.05).

potential into neural lineages (Figure 6.4G, H). However, the cells at this stage can still differentiate into SMCs, chondrocytes, osteoblasts and adipocytes

(Figure 6.4I-L), suggesting a neural crest to mesenchymal transition process during the differentiation. In addition, it is likely that previously identified synovial MSCs are partially differentiated NCCL-SSCs in undefined medium.

6.6 Effects of porosity on lineage specification of NCCL-SSCs

Although cell infiltration is favored to produce three-dimensional tissues, whether it is appropriate for stem cells to differentiate into different lineages is not well understood. Therefore, we cultured the NCCL-SSCs on scaffolds with varying porosity using spontaneous differentiation media without any specific chemical clues for 1 week and analyzed the lineage marker expressions. The PLLA scaffold (low porosity) and PLLA/PGA scaffold degraded for 4 weeks with highest porosity were selected to directly compare whether specific lineages favor certain pore size. qPCR revealed that mRNA level of aggrecan for cells seeded on highly porous PLLA/PGA scaffold was increased by 3.6-fold compared to that of cells seeded on the much less porous PLLA scaffold (Figure 6.5A). Likewise, mRNA level of collagen II was also increased by 2.67-fold (Figure 6.5B), indicating that higher porosity may be more favorable for NCCL-SSCs to differentiate into chondrocytes. In addition, mRNA level of bone markers including osteocalcin and Runx2 were increased 2.23-fold and 1.97-fold respectively (Figure 6.5C, D), indicating that large pore size may also favor osteoblast differentiation. In contrast, SMC markers including SMA and CNN1 were decreased by 10.5-fold and 4.32-fold respectively (Figure 6.5E, F). Adipogenic markers including LPL and PPARg were also decreased by 4.04-fold and 12.2-fold respectively (Figure 6.5G, H), indicating that NCCL-SSC differentiation into SMC and adipocytes may favor scaffolds with lower porosity.

6.7 Conclusion

In this study, we identified precursors of synovial MSCs, which have multipotency into both ectodermal and mesenchymal lineages. Various transcriptional factors including Sox10 and Sox17 can be used to characterize this type of stem cells despite the widely surface markers. Moreover, the neural crest to mesenchymal transition of NCCL-SSCs identified in this study might represent a general mechanism for adult stem cell differentiation. This study shows that different porosity of scaffold might be favorable according to the targeted lineage, thus providing guidance for designing of desirable scaffold for tissue engineering and regenerative medicine.

Chapter 7. Discussion

This dissertation work identified a novel type of adult stem cells with neural crest cell characteristics resident in different tissues all over the body. We first discovered it in blood vessel wall in Chapter 2 and elucidated its function and the relationship with previously blamed cell types behind vascular diseases such as restenosis and atherosclerosis. The identification of MVSCs brings a new perspective on vascular remodeling and disease development. In Chapter 3, our *in vitro* experiments suggest that proliferative/synthetic SMCs are derived from the differentiation of MVSCs instead of the de-differentiation of contractile SMCs. *In vivo* experiments also demonstrate that MVSCs, rather than mature SMCs, repopulate the tunica media and form neointima after endothelial denudation injury. These results provide the first direct evidence to support the MVSC differentiation hypothesis and disprove the SMC de-differentiation theory. The fact that highly expandable and migratory MVSCs were not derived from mature SMCs suggests that the previously reported decrease of contractile markers in SMC culture *in vitro* or after vascular injury *in vivo* could be attributed to the rapid expansion of MVSCs and their spontaneous differentiation into immature SMCs. MVSCs not only proliferate and differentiate, but also become synthetic and secrete matrix proteins such as collagen I, collagen II and aggrecan. The potentials of MVSC differentiation into SMCs, chondrogenic cells and other lineages offers a novel and reasonable explanation for the complex phenotypes of cells in the diseased vessel.

MVSCs at different stages of differentiation could also explain the heterogeneity of SMCs in culture and *in vivo*. The fact that MVSCs and their derivatives respond differently to vascular growth factors underscores the importance of characterization of cell culture from blood vessels. In the literature, the differentiation stage of “SMCs” is usually not well characterized. For example, the cells positive for SMA, SM-22α and CNN1 are often treated as SMCs rather than immature SMCs or partially differentiated MVSCs. In many studies, the cells in culture may not be homogeneous at a specific differentiation stage, which may result in conflicting observations and explanation. Previous studies have identified a subpopulation of SMCs, termed “epithelioid” cells, from newborn or injured vessels [76,77,78,79]. The origin of these SMCs is not known, and the relationship of “epithelioid” cells with vascular stem cells has not been explored. It is very likely that “epithelioid” SMCs are derived from MVSCs. However, in adults, MVSCs can be isolated from both normal vessels and injured vessels, but “epithelioid” SMCs are only derived from injured vessels. It is possible that dormant MVSCs are a small population in normal vessels and may be overlooked.

In addition to proliferative/synthetic SMCs, MVSCs could differentiate into mature SMCs (SM-MHC$^+$) *in vitro* and *in vivo*. It is also worth noting that the extent of MVSC activation, proliferation and differentiation could be dependent

on the extent of vascular injury and SMC damage[56]. Another important finding is that MVSCs are the cell type in blood vessel wall that can be activated by vascular injury to proliferate and participate in remodeling. Neointima cells have a large cell body, secrete extra-cellular matrix (ECM) and express lower levels of the smooth muscle-specific contractile proteins [80], which is consistent with our findings on the changes of cell morphology and the expression of SMC markers during the spontaneous differentiation of MVSCs. In this study, we showed that MVSCs, instead of SMCs, are the major cell type in neointimal tissue as characterized by MVSC makers. Given the fact that some MVSCs in neointima still retain multipotency, it is reasonable to propose that aberrant activation, expansion and differentiation of MVSCs may contribute to not only SMC differentiation and cartilage formation but also many other aspects of vascular diseases such as fat and cholesterol metabolism, matrix remodeling and calcification. Since the rodent model of denudation injury does not result in significant fat and cholesterol accumulation and intima calcification, the possibility of MVSC differentiation into adipogenic and osteogenic cells in diseased vessels remains to be tested by using atherosclerosis models. The identification of MVSC in human arteries in Chapter 4 makes MVSC a potential therapeutic target of vascular diseases.

To date, MVSCs are a unique precursor identified for adult MSCs and MSC-like cells, and it is likely that MSC precursors similar to MVSCs may exist in many other tissues. MVSCs express CD29 and CD44, two non-specific surface markers of MSCs and SMCs. However, there was no specific marker, especially transcriptional factor marker, for MSCs. In this study, we have identified several transcriptional markers and cytoskeletal markers in MVSCs, e.g., Sox17, Sox10, nestin, NFM and S100β. In addition, we showed that MSC-like cells were also positive for some of these markers (except Sox17). These results provide insight into the characteristics of MVSCs and MSC-like cells, not only in blood vessels, but also in other tissue types. In Chapter 5, we also identified this type of stem cells not only in blood vessel wall, but also in the facial tissues under dermis. Similarly, this type of stem cells respond rapidly to injury and can be activate to proliferate to participate into the tissue remodeling, like artificial vascular grafts, implanted biomaterials and general wound healing.

In the wound healing process, myofibroblasts were identified as the main cell type in wound healing. Despite their importance in wound healing and scar formation, fibroblasts and myofibroblasts are mainly characterized by cell morphology, ultra-structures including extensive cell-matrix adhesion, abundant intercellular adherens and bundles of contractile cytoplasmic microfilaments such as non-muscle myosin[68]. To date, there is no detailed characterization such as transcriptome, specific surface markers as well as the suitable culture condition to maintain specific phenotype. In chapter 6, we found the precursor of myofibroblasts that participated in the general dermal wound healing as well as tissue engineered scaffolds. This type of stem cells

could spontaneously differentiate into myofibroblasts *in vitro* and *in vivo* to form the capsule layer around skin wound and transplanted biomaterials. More importantly, we performed detailed characterization, thus providing new insight into the myofibroblast biology as well as wound healing.

Besides the general wound healing and vascular remodeling, we also identified this type of stem cells in joint synovial tissue in Chapter 6. This new discovery not only renews our understanding of adult stem cells, but also provides useful tools for further investigation of knee joint specific stem cells. The neural crest to mesenchymal transition of NCCL-SSCs might also represent a general mechanism of adult stem cell differentiation.

Since efficient stem cell differentiation into specific lineage is essential requirement for tissue regeneration, scaffolds with desirable properties that can facilitate directed stem cell differentiation is favored. Although scaffolds with large pore size and high porosity are generally favored to promote cell infiltration for three-dimensional tissue engineering, there is limited studies available indicating whether it is advantageous for specific lineages. Even though there are reports that pore size of scaffolds can influence stem cell differentiation towards certain lineage [81,82,83,84], the lack of a systematic study using one single stem cell type with multiple types of targeted lineages makes it hard to prove the concept. Here, we demonstrated the effects of increased porosity and enhanced cell infiltration on lineage specification of NCCL-SSCs without specific chemical cues, indicating that certain properties of scaffolds can be utilized and tailored to regulate stem cell behaviors. Our finding demonstrating that different lineages may favor scaffolds with different porosity provides knowledge on better selecting appropriate scaffolds for tissue engineering of desired tissues types.

In summary, this dissertation work discovered a novel type of stem cells and identified many transcription factors as well as surface markers and various specific properties, which provided new insight into adult stem cells. More importantly, we demonstrated the function of this type of stem cells in tissue remodeling and disease development in the cardiovascular system, general wound healing process, and joint synovial tissues. Our results revealed the ‘dark side’ of adult stem cells such as the contribution to neointimal hyperplasia, blood vessel hardening and fibrosis and suggest that stem cells might be the target for drug screening for various diseases. In addition, our study also highlighted the importance of stem cell niche such as topographical guidance and physical properties. Efforts towards engineering a regenerative stem cell niche might represent another novel approach for functional tissue engineering. Overall, we hope this study could shed light and promote much work in the field of regenerative medicine, thus benefiting our healthcare system.

References

1. (1997) The sixth report of the Joint National Committee on prevention, detection, evaluation, and treatment of high blood pressure. Arch Intern Med 157: 2413-2446.
2. Ara S (2004) A literature review of cardiovascular disease management programs in managed care populations. J Manag Care Pharm 10: 326-344.
3. Kwon GP, Schroeder JL, Amar MJ, Remaley AT, Balaban RS (2008) Contribution of macromolecular structure to the retention of low-density lipoprotein at arterial branch points. Circulation 117: 2919-2927.
4. Hansson GK, Hermansson A (2011) The immune system in atherosclerosis. Nat Immunol 12: 204-212.
5. Giordano A, Romano A (2011) Inhibition of human in-stent restenosis: a molecular view. Curr Opin Pharmacol 11: 372-377.
6. Costa MA, Simon DI (2005) Molecular basis of restenosis and drug-eluting stents. Circulation 111: 2257-2273.
7. Owens GK, Kumar MS, Wamhoff BR (2004) Molecular regulation of vascular smooth muscle cell differentiation in development and disease. Physiol Rev 84: 767-801.
8. Owens GK (1995) Regulation of differentiation of vascular smooth muscle cells. Physiol Rev 75: 487-517.
9. Chamley-Campbell J, Campbell GR, Ross R (1979) The smooth muscle cell in culture. Physiol Rev 59: 1-61.
10. Buck R (1961) Intimal Thickening After Ligature of Arteries An Electron-Microscopic Study. Circ Res 9: 418-426.
11. Kretzschmar K, Watt FM (2012) Lineage tracing. Cell 148: 33-45.
12. Naik V, Leaf EM, Hu JH, Yang HY, Nguyen NB, et al. (2012) Sources of cells that contribute to atherosclerotic intimal calcification: an in vivo genetic fate mapping study. Cardiovasc Res 94: 545-554.
13. Wamhoff BR, Hoofnagle MH, Burns A, Sinha S, McDonald OG, et al. (2004) A G/C element mediates repression of the SM22alpha promoter within phenotypically modulated smooth muscle cells in experimental atherosclerosis. Circ Res 95: 981-988.
14. Regan CP, Adam PJ, Madsen CS, Owens GK (2000) Molecular mechanisms of decreased smooth muscle differentiation marker expression after vascular injury. J Clin Invest 106: 1139-1147.
15. Speer MY, Yang HY, Brabb T, Leaf E, Look A, et al. (2009) Smooth muscle cells give rise to osteochondrogenic precursors and chondrocytes in calcifying arteries. Circ Res 104: 733-741.
16. Faggin E, Puato M, Zardo L, Franch R, Millino C, et al. (1999) Smooth muscle-specific SM22 protein is expressed in the adventitial cells of balloon-injured rabbit carotid artery. Arterioscler Thromb Vasc Biol 19: 1393-1404.
17. Iwata H, Manabe I, Fujiu K, Yamamoto T, Takeda N, et al. (2010) Bone marrow-derived cells contribute to vascular inflammation but do not differentiate into smooth muscle cell lineages. Circulation 122: 2048-2057.
18. Huang NF, Patel S, Thakar RG, Wu J, Hsiao BS, et al. (2006) Myotube assembly on nanofibrous and micropatterned polymers. Nano Lett 6: 537-542.

19. Patel S, Kurpinski K, Quigley R, Gao H, Hsiao BS, et al. (2007) Bioactive nanofibers: synergistic effects of nanotopography and chemical signaling on cell guidance. Nano Lett 7: 2122-2128.
20. Hashi CK, Zhu Y, Yang GY, Young WL, Hsiao BS, et al. (2007) Antithrombogenic property of bone marrow mesenchymal stem cells in nanofibrous vascular grafts. Proc Natl Acad Sci U S A 104: 11915-11920.
21. Kurpinski KT, Stephenson JT, Janairo RR, Lee H, Li S (2010) The effect of fiber alignment and heparin coating on cell infiltration into nanofibrous PLLA scaffolds. Biomaterials 31: 3536-3542.
22. Hashi CK, Derugin N, Janairo RR, Lee R, Schultz D, et al. Antithrombogenic Modification of Small-Diameter Microfibrous Vascular Grafts. Arteriosclerosis Thrombosis and Vascular Biology.
23. Tang Z, Wang A, Yuan F, Yan Z, Liu B, et al. (2012) Differentiation of multipotent vascular stem cells contributes to vascular diseases. Nat Commun 3: 875.
24. Wang A, Tang Z, Park IH, Zhu Y, Patel S, et al. (2011) Induced pluripotent stem cells for neural tissue engineering. Biomaterials 32: 5023-5032.
25. Descalzi D, Folli C, Scordamaglia F, Riccio AM, Gamalero C, et al. (2007) Importance of fibroblasts-myofibroblasts in asthma-induced airway remodeling. Recent Pat Inflamm Allergy Drug Discov 1: 237-241.
26. Lorena D, Uchio K, Costa AM, Desmouliere A (2002) Normal scarring: importance of myofibroblasts. Wound Repair Regen 10: 86-92.
27. Friedenstein AJ, Chailakhjan RK, Lalykina KS (1970) The development of fibroblast colonies in monolayer cultures of guinea-pig bone marrow and spleen cells. Cell Tissue Kinet 3: 393-403.
28. Luria EA, Panasyuk AF, Friedenstein AY (1971) Fibroblast colony formation from monolayer cultures of blood cells. Transfusion 11: 345-349.
29. Iwano M, Plieth D, Danoff TM, Xue C, Okada H, et al. (2002) Evidence that fibroblasts derive from epithelium during tissue fibrosis. J Clin Invest 110: 341-350.
30. Ogawa M, LaRue AC, Drake CJ (2006) Hematopoietic origin of fibroblasts/myofibroblasts: Its pathophysiologic implications. Blood 108: 2893-2896.
31. Kraus VB (1997) Pathogenesis and treatment of osteoarthritis. Med Clin North Am 81: 85-112.
32. De Bari C, Dell'Accio F, Tylzanowski P, Luyten FP (2001) Multipotent mesenchymal stem cells from adult human synovial membrane. Arthritis Rheum 44: 1928-1942.
33. Mendelson A, Frank E, Allred C, Jones E, Chen M, et al. (2011) Chondrogenesis by chemotactic homing of synovium, bone marrow, and adipose stem cells in vitro. FASEB J 25: 3496-3504.
34. Lee CH, Cook JL, Mendelson A, Moioli EK, Yao H, et al. (2010) Regeneration of the articular surface of the rabbit synovial joint by cell homing: a proof of concept study. Lancet 376: 440-448.
35. Lannutti J, Reneker D, Ma T, Tomasko D, Farson D (2007) Electrospinning for tissue engineering scaffolds. Materials Science and Engineering: C 27: 504-509.
36. Tan SH, Inai R, Kotaki M, Ramakrishna S (2005) Systematic parameter study for ultra-fine fiber fabrication via electrospinning process. Polymer 46: 6128-6134.

37. Jang JH, Castano O, Kim HW (2009) Electrospun materials as potential platforms for bone tissue engineering. Adv Drug Deliv Rev 61: 1065-1083.
38. Bhattarai SR, Bhattarai N, Yi HK, Hwang PH, Cha DI, et al. (2004) Novel biodegradable electrospun membrane: scaffold for tissue engineering. Biomaterials 25: 2595-2602.
39. Steitz SA, Speer MY, Curinga G, Yang HY, Haynes P, et al. (2001) Smooth muscle cell phenotypic transition associated with calcification: upregulation of Cbfa1 and downregulation of smooth muscle lineage markers. Circ Res 89: 1147-1154.
40. Siow RC, Pearson JD (2001) Vascular smooth muscle cells : isolation, culture, and characterization. Methods Mol Med 46: 237-245.
41. Lee G, Kim H, Elkabetz Y, Al Shamy G, Panagiotakos G, et al. (2007) Isolation and directed differentiation of neural crest stem cells derived from human embryonic stem cells. Nat Biotechnol 25: 1468-1475.
42. Hashi CK, Derugin N, Janairo RR, Lee R, Schultz D, et al. (2010) Antithrombogenic modification of small-diameter microfibrous vascular grafts. Arterioscler Thromb Vasc Biol 30: 1621-1627.
43. Zhu Y, Wang A, Patel S, Kurpinski K, Diao E, et al. (2011) Engineering bi-layer nanofibrous conduits for peripheral nerve regeneration. Tissue engineering Part C, Methods 17: 705-715.
44. Huang NF, Kurpinski K, Fang Q, Lee RJ, Li S (2011) Proteomic identification of biomarkers of vascular injury. Am J Transl Res 3: 139-148.
45. Churchman AT, Siow RC (2009) Isolation, culture and characterisation of vascular smooth muscle cells. Methods Mol Biol 467: 127-138.
46. Crisan M, Yap S, Casteilla L, Chen CW, Corselli M, et al. (2008) A perivascular origin for mesenchymal stem cells in multiple human organs. Cell Stem Cell 3: 301-313.
47. Hu Y, Zhang Z, Torsney E, Afzal AR, Davison F, et al. (2004) Abundant progenitor cells in the adventitia contribute to atherosclerosis of vein grafts in ApoE-deficient mice. J Clin Invest 113: 1258-1265.
48. Sainz J, Al Haj Zen A, Caligiuri G, Demerens C, Urbain D, et al. (2006) Isolation of "side population" progenitor cells from healthy arteries of adult mice. Arterioscler Thromb Vasc Biol 26: 281-286.
49. Medici D, Shore EM, Lounev VY, Kaplan FS, Kalluri R, et al. (2010) Conversion of vascular endothelial cells into multipotent stem-like cells. Nat Med 16: 1400-1406.
50. Marion NW, Mao JJ (2006) Mesenchymal stem cells and tissue engineering. Methods Enzymol 420: 339-361.
51. Molofsky AV, Pardal R, Iwashita T, Park IK, Clarke MF, et al. (2003) Bmi-1 dependence distinguishes neural stem cell self-renewal from progenitor proliferation. Nature 425: 962-967.
52. Tintut Y, Alfonso Z, Saini T, Radcliff K, Watson K, et al. (2003) Multilineage potential of cells from the artery wall. Circulation 108: 2505-2510.
53. Abedin M, Tintut Y, Demer LL (2004) Mesenchymal stem cells and the artery wall. Circ Res 95: 671-676.
54. Clowes AW, Schwartz SM (1985) Significance of quiescent smooth muscle migration in the injured rat carotid artery. Circ Res 56: 139-145.
55. Clowes AW, Reidy MA, Clowes MM (1983) Kinetics of cellular proliferation after arterial

injury. I. Smooth muscle growth in the absence of endothelium. Lab Invest 49: 327-333.

56. Fingerle J, Au YP, Clowes AW, Reidy MA (1990) Intimal lesion formation in rat carotid arteries after endothelial denudation in absence of medial injury. Arteriosclerosis 10: 1082-1087.
57. Madsen CS, Regan CP, Hungerford JE, White SL, Manabe I, et al. (1998) Smooth muscle-specific expression of the smooth muscle myosin heavy chain gene in transgenic mice requires 5'-flanking and first intronic DNA sequence. Circ Res 82: 908-917.
58. Xin HB, Deng KY, Rishniw M, Ji G, Kotlikoff MI (2002) Smooth muscle expression of Cre recombinase and eGFP in transgenic mice. Physiol Genomics 10: 211-215.
59. Nguyen AT, Gomez D, Bell RD, Campbell JH, Clowes AW, et al. (2012) Smooth Muscle Cell Plasticity: Fact or Fiction? Circ Res.
60. Yu J, Wang A, Tang Z, Henry J, Li-Ping Lee B, et al. (2012) The effect of stromal cell-derived factor-1alpha/heparin coating of biodegradable vascular grafts on the recruitment of both endothelial and smooth muscle progenitor cells for accelerated regeneration. Biomaterials 33: 8062-8074.
61. Belteki G, Haigh J, Kabacs N, Haigh K, Sison K, et al. (2005) Conditional and inducible transgene expression in mice through the combinatorial use of Cre-mediated recombination and tetracycline induction. Nucleic Acids Res 33: e51.
62. Cuttler AS, LeClair RJ, Stohn JP, Wang Q, Sorenson CM, et al. (2011) Characterization of Pdgfrb-Cre transgenic mice reveals reduction of ROSA26 reporter activity in remodeling arteries. Genesis 49: 673-680.
63. Kurpinski K, Lam H, Chu J, Wang A, Kim A, et al. (2010) Transforming growth factor-beta and notch signaling mediate stem cell differentiation into smooth muscle cells. Stem Cells 28: 734-742.
64. Malik N, Francis SE, Holt CM, Gunn J, Thomas GL, et al. (1998) Apoptosis and cell proliferation after porcine coronary angioplasty. Circulation 98: 1657-1665.
65. Bennett MR (1999) Apoptosis of vascular smooth muscle cells in vascular remodelling and atherosclerotic plaque rupture. Cardiovasc Res 41: 361-368.
66. Yang S (2012) The real culprit behind hardened arteries? Stem cells, says landmark study. UC Berkeley News
67. Tang Z, Wang A, Wang D, Li S (2012) Smooth Muscle Cells: To Be or Not To Be? Response to Nguyen et al. Circ Res.
68. Tomasek JJ, Gabbiani G, Hinz B, Chaponnier C, Brown RA (2002) Myofibroblasts and mechano-regulation of connective tissue remodelling. Nat Rev Mol Cell Biol 3: 349-363.
69. Ross R, Everett NB, Tyler R (1970) Wound healing and collagen formation. VI. The origin of the wound fibroblast studied in parabiosis. J Cell Biol 44: 645-654.
70. Hinz B, Phan SH, Thannickal VJ, Galli A, Bochaton-Piallat ML, et al. (2007) The myofibroblast: one function, multiple origins. Am J Pathol 170: 1807-1816.
71. Lee BL, Jeon H, Wang A, Yan Z, Yu J, et al. (2012) Femtosecond laser ablation enhances cell infiltration into three-dimensional electrospun scaffolds. Acta Biomater 8: 2648-2658.

72. Janairo RR, Henry JJ, Lee BL, Hashi CK, Derugin N, et al. (2012) Heparin-modified small-diameter nanofibrous vascular grafts. IEEE Trans Nanobioscience 11: 22-27.
73. Rooker SM, Liu B, Helms JA (2010) Role of Wnt signaling in the biology of the periodontium. Dev Dyn 239: 140-147.
74. Nimura A, Muneta T, Koga H, Mochizuki T, Suzuki K, et al. (2008) Increased proliferation of human synovial mesenchymal stem cells with autologous human serum: comparisons with bone marrow mesenchymal stem cells and with fetal bovine serum. Arthritis Rheum 58: 501-510.
75. Fan J, Varshney RR, Ren L, Cai D, Wang DA (2009) Synovium-derived mesenchymal stem cells: a new cell source for musculoskeletal regeneration. Tissue Eng Part B Rev 15: 75-86.
76. Bochaton-Piallat ML, Ropraz P, Gabbiani F, Gabbiani G (1996) Phenotypic heterogeneity of rat arterial smooth muscle cell clones. Implications for the development of experimental intimal thickening. Arterioscler Thromb Vasc Biol 16: 815-820.
77. Adams LD, Lemire JM, Schwartz SM (1999) A systematic analysis of 40 random genes in cultured vascular smooth muscle subtypes reveals a heterogeneity of gene expression and identifies the tight junction gene zonula occludens 2 as a marker of epithelioid "pup" smooth muscle cells and a participant in carotid neointimal formation. Arterioscler Thromb Vasc Biol 19: 2600-2608.
78. Lemire JM, Covin CW, White S, Giachelli CM, Schwartz SM (1994) Characterization of cloned aortic smooth muscle cells from young rats. Am J Pathol 144: 1068-1081.
79. Kocher O, Gabbiani F, Gabbiani G, Reidy MA, Cokay MS, et al. (1991) Phenotypic features of smooth muscle cells during the evolution of experimental carotid artery intimal thickening. Biochemical and morphologic studies. Lab Invest 65: 459-470.
80. Christen T, Verin V, Bochaton-Piallat M, Popowski Y, Ramaekers F, et al. (2001) Mechanisms of neointima formation and remodeling in the porcine coronary artery. Circulation 103: 882-888.
81. Sicchieri LG, Crippa GE, de Oliveira PT, Beloti MM, Rosa AL (2012) Pore size regulates cell and tissue interactions with PLGA-CaP scaffolds used for bone engineering. J Tissue Eng Regen Med 6: 155-162.
82. Oh SH, Kim TH, Im GI, Lee JH (2010) Investigation of pore size effect on chondrogenic differentiation of adipose stem cells using a pore size gradient scaffold. Biomacromolecules 11: 1948-1955.
83. Kasten P, Beyen I, Niemeyer P, Luginbuhl R, Bohner M, et al. (2008) Porosity and pore size of beta-tricalcium phosphate scaffold can influence protein production and osteogenic differentiation of human mesenchymal stem cells: an in vitro and in vivo study. Acta Biomater 4: 1904-1915.
84. Im GI, Ko JY, Lee JH (2012) Chondrogenesis of adipose stem cells in a porous polymer scaffold: influence of the pore size. Cell Transplant.